

Testing the Local Martingale Theory of Bubbles using Cryptocurrencies^{*}

Soon Hyeok Choi[†] Robert A. Jarrow[‡]

April 2021

[Click here for the most recent version](#)

Abstract

Cryptocurrencies provide the ideal and natural experimental setting to test the local martingale theory of bubbles, because they have no cash flows. Using this theory, we test for the existence of price bubbles in eight cryptocurrencies from January 1, 2019 to July 17, 2019. The cryptocurrencies are Bitcoin (BTC), Litecoin (LTC), Ethereum (ETH), Ripple (XRP), Bitcoin Cash (BCH), EOS (EOS), Monero (XMR), and Zcash (ZEC). A novel, simple, and robust testing methodology is created to facilitate this estimation. During this time frame, five of the eight currencies (BTC, BCH, EOS, XMR, ZEC) exhibit price bubbles, Litecoin does not, and the evidence for Ethereum and Ripple is inconclusive. The paper provides strong evidence for the prevalence of bubbles in cryptocurrencies and supports the feasibility of applying the local martingale theory of bubbles to various asset classes.

Keywords: Price Bubbles, Cryptocurrency, Martingale

JEL Codes: G12, G13, G14, G17, G18

^{*}We thank Warren Bailey, Crocker Liu, William Cong. We received helpful comments from participants at the Korea Association of Financial Engineering and Korea Derivatives Association.

[†]School of Hotel Administration, SC Johnson College of Business, Cornell University, Ithaca, N.Y. 14853. ✉ sc983@cornell.edu.

[‡]Samuel Curtis Johnson Graduate School of Management, Cornell University, Ithaca, N.Y. 14853 and Kamakura Corporation, Honolulu, Hawaii 96815. ✉ raj15@cornell.edu.

Contents

1	Introduction	1
2	The Local Martingale Theory of Bubbles	5
2.1	Set-Up	5
2.2	The Fundamental Value	6
2.3	Type 3 Bubbles	7
2.4	The Testing Methodology	7
2.4.1	The Cryptocurrency's Price Process	8
2.4.2	The Bubble Test	8
3	The Empirical Methodology	9
3.1	Data	10
3.1.1	Source	10
3.1.2	Description	10
3.2	Volatility Estimation	12
3.2.1	The Florens-Zmirou Estimator	12
3.2.2	Estimation Results	13
3.3	Interpolation	14
3.4	Extrapolation and Evaluation	15
3.5	Discussion	19
4	Results	20
5	Robustness Tests	22
5.1	Outlier Analysis	22
5.2	Foreign Exchange Rates	24
6	Conclusion	27
	References	29

Appendices	32
A Modified Convex Hull Algorithm (MCHA)	32
B Hypothesis Testing	36
C Data Diagnostics	37
D Volatility Estimation Results	41
E Interpolation (Cryptocurrency)	45
F Interpolation (Crypto, Winsorized)	50
G Extrapolation (Cryptocurrency)	55
H Interpolation (Foreign Currency)	60
I Interpolation (FOREX, Winsorized)	63
J Extrapolation (Foreign Currency)	66
K Extrapolation: Regression (Crypto, FOREX)	69
L Extrapolation: Regression (Crypto, Winsorized)	74
M Extrapolation: Regression (FOREX, Winsorized)	77
N Extrapolation (FOREX, Winsorized)	79
O Extrapolation (Crypto, Winsorized)	82

1 Introduction

There is a rich economics literature concerning asset price bubbles using historical time series data in a discrete time and infinite horizon setting (see [Brunnermeier and Oehmke \[2013\]](#) for a survey). As discussed in [Jarrow et al. \[2010\]](#), in the most general model structure possible, there are three types of bubbles: *type 1*, *type 2*, and *type 3*. A type 1 bubble exists only in infinite horizon models, and it captures a bubble in fiat money, a security with zero cash flows, but strictly positive value. A type 2 bubble also exists only in infinite horizon models, and it corresponds to an asset whose price process (under the risk neutral probability measure) is a martingale but not a uniformly integrable martingale. Intuitively, the sum of the risk adjusted expected discounted cash flows and liquidation value at time *infinity* (i.e. the asset's fundamental value) does not equal the market price. Finally, a type 3 bubble exists only in continuous trading models, and it corresponds to an asset whose price process is a local martingale, but not a martingale. In economic terms, the risk adjusted expected discounted cash flows and liquidation value at some finite time horizon does not equal the market price. This translates to the asset's fundamental value not being equal to its market price. We study *type 3* bubbles in this paper while the aforementioned literature focuses on *type 2* bubbles.

It is important to note that type 2 and 3 bubbles capture different economic phenomena. Type 2 bubbles are studied within an infinite horizon model where the market price of an asset is compared to its fundamental value and estimated using a model for the asset's dividends and discount rate. There are two problems with these models, which explain why the evidence for the existence of type 2 asset price bubbles is mixed. First, since the model is infinite horizon, the model estimation requires a large time series sample, which creates a problem when there are structural breaks or non-stationarities in financial markets. Second, as there is no consensus on the model for an asset's fundamental value, there is a joint hypothesis issue.

In contrast, a type 3 bubble exists because investors attempt to capture

short-term trading profits via buying and selling over some fixed and finite horizon, an example being high frequency trading. A type 3 bubble exists when the market price for an asset exceeds its fundamental value where the asset’s fundamental value can be interpreted as the price paid for the asset to buy and hold (i.e. without resale) until liquidation. That is, there are no type 3 bubbles when the market price equals its buy and hold value. Equally as important, [Jarrow et al. \[2011b,a\]](#) show it is possible to test for the existence of type 3 bubbles without estimating an asset’s fundamental value, thereby avoiding the joint hypothesis issue. This paper tests for the existence of type 3 bubbles in cryptocurrency markets.

The theory surrounding the existence of type 3 bubbles is called the *local martingale theory of bubbles*. Cryptocurrency markets provide the “perfect and natural experiment” to test this local martingale theory of bubbles. The reason is that cryptocurrencies have no cash flows; the fundamental value corresponds to the currency’s liquidation value at the model’s horizon. This implies that bubbles exist in cryptocurrencies when speculators buy to resell before the model’s horizon. This seems very likely for these new assets. Indeed, since the purpose of many cryptocurrencies is to serve as a medium of exchange,¹ in theory, if purchased to buy and hold and to use as needed, the transaction demand for these assets should be constrained by the usage of other more standard currencies to execute transactions. In contrast to this expectation, the recent expansion of the cryptocurrency market has been extraordinary. In January 2016, Bitcoin’s market capitalization was at \$15 million dollars, and on December 17 2017, it reached \$334 billion. In two years, its market capitalization grew 22,000 fold. And, just as abruptly, in 2018 Bitcoin’s market capitalization decreased to a mere \$6 billion to which many argue reflects Bitcoin’s “bubble” bursting. See [Geuder et al. \[2019\]](#) and [Cheah and Fry \[2015\]](#) who investigate the presence of price bubbles in

¹Cryptocurrencies can be divided into four different types: general payment tokens, platform tokens, product tokens, and cash-flow tokens. The use of cryptocurrencies as a medium of exchange applies mostly to general payment tokens or platform tokens that have a large outstanding volume. See [Cong et al. \[2020b\]](#).

Bitcoin. [Bouri et al. \[2019\]](#) argue that the cryptocurrency market is prone to herding behavior, and they find evidence of a high degree of co-movement in the cross-sectional returns across different cryptocurrencies.

One major concern associated with cryptocurrencies is their vulnerability to price manipulation. Using the 2017 blockchain data, [Griffin and Shams \[2019\]](#) find that Tether’s purchases are often timed following market downturns to directly influence Bitcoin’s price, thereby generating profitable trading strategies across the two currencies. [Li et al. \[2019\]](#) investigate pump-and-dump schemes (P&Ds) in cryptocurrency markets and discover that most P&Ds lead to short-term bubbles where prices, volume, and volatility increase significantly followed by a rapid reversion. [Cong et al. \[2020a\]](#) find significant false transactions known as wash trading in twenty nine different cryptocurrency exchanges.

The local martingale theory of bubbles used in this paper is consistent with testing for cryptocurrency bubbles regardless of the activities generating them: speculation or manipulation. The model applies to an econometrician or trader, who uses price data to estimate bubbles and views themselves as a price-taker with respect to trading in these markets. This theory can be tested by examining the market price process to see whether it is a local martingale or a martingale under the risk neutral (equivalent martingale) probabilities. These two processes have different local characteristics, which can be estimated without computing the asset’s fundamental value.

The testing methodology is as follows. Given an observed price evolution over a fixed time interval, one estimates the price process’s volatility as a function of the asset’s price level. This estimation produces a set of volatility and price pairs. The key step is to check to see if a certain integral of this volatility function is finite or not when computed over the entire non-negative real line. This step requires extrapolating the volatility function from the observed price interval to the entire non-negative real line. [Jarrow et al. \[2011b,a\]](#) employ a non-parametric approach to perform the volatility estimation, and then given the estimated volatility and price pairs, extrapol-

ate using the theory of Reproducing Kernel Hilbert Spaces (RKHS). [Chaim and Laurini \[2019\]](#) also use this approach to examine the presence of bubbles in Bitcoin.

In contrast, we introduce a different interpolation and extrapolation technique based on the modified convex hull of the estimated volatility and price pairs to provide upper and lower bounds on this integral’s value. This is the second contribution of our paper. Our method is robust and simple to implement, and it is successful in identifying price bubbles. Indeed, using this approach we test for the existence of bubbles in eight different cryptocurrencies from January 1, 2019 to July 17, 2019. The cryptocurrencies are Bitcoin (BTC), Litecoin (LTC), Ethereum (ETH), Ripple (XRP), Bitcoin Cash (BCH), EOS (EOS), Monero (XMR), and Zcash (ZEC). We document that five of the eight cryptocurrencies exhibit bubbles, LTC does not, and ETH and XRP are inconclusive. This is strong evidence supporting the existence of price bubbles in cryptocurrencies and equally strong evidence supporting the validity of the local martingale theory of bubbles.

As a robustness test, to control for the standard errors of the volatility estimates, we winsorize them by replacing the largest and smallest volatilities with the second largest and smallest volatility estimates. Repeating the hypothesis testing, the conclusions are identical with the exception of XRP. After the winsorization, the hypothesis test for XRP is inconclusive, whereas before it indicated a bubble. This robustness test confirms the validity of our empirical methodology.

As a second robustness test of the methodology constructed herein, we also apply our methodology to see if bubbles exist in four standard foreign currencies over the same time period. The four currencies are the Japanese Yen, Great British Pound, Canadian Dollar, and Euro. The evidence indicates that the Great British Pound exhibits a bubble while there is no bubble in the Japanese Yen. The evidence for the existence of bubbles in the Canadian Dollar and the Euro is inconclusive. This robustness test further supports the validity of the local martingale theory of bubbles and provides

an alternative perspective on the use of foreign currencies for speculative purposes.

This paper also has important policy implications for cryptocurrencies. There has been increasingly aggressive penetration of cryptocurrencies into the market potentially for commercial use. Indeed, Facebook continues to invest tremendous resources in launching its cryptocurrency, Libra. And, in March 2020, Microsoft filed a patent for new cryptocurrency system using body activity data. Whether or not the commercial use of these currencies will exceed their use for speculative is an open question. If cryptocurrencies uniformly exhibit price bubbles, which appears to be the case from our limited study, then their use for speculation dominates their use as a medium of exchange (especially given the standard alternatives), and perhaps their introduction should be prohibited. We note that to help regulate these markets and reduce harmful speculation, the US Congress recently introduced the Virtual Currency Tax Fairness Act of 2020.

An outline of this paper is as follows. Section 2 reviews the local martingale theory of bubbles and section 3 describes the empirical methodology. Section 4 presents the results, section 5 presents two robustness tests, and section 6 concludes.

2 The Local Martingale Theory of Bubbles

This section reviews the local martingale theory of bubbles in order to understand the testing methodology employed for bubble detection.

2.1 Set-Up

We assume a continuous time model over the finite horizon $[0, T]$. Given is a filtered probability space $(\Omega, \mathcal{F}, F = (\mathcal{F}_t)_{t \in [0, T]}, \mathbb{P})$ satisfying the usual hypotheses where Ω is the state space, \mathcal{F} is a σ -algebra of events, $F = (\mathcal{F}_t)_{t \in [0, T]}$ is an information filtration, and \mathbb{P} is the statistical probability measure (see [Protter \[2005\]](#) for the relevant definitions).

We assume traded continuously, in a frictionless and competitive market, are a default-free money market account (mma) and a cryptocurrency. *Frictionless* means there are neither transaction costs nor trading constraints. *Competitive* means that the trader (using this model) believes that she can buy and sell the traded assets without affecting their prices. Without loss of generality, we assume that the mma has unit value at all times. We denote the normalized market price of the cryptocurrency by S_t , assumed to be a semimartingale with respect to F .

We suppose that the market is arbitrage-free.² Hence, by the First Fundamental Theorem of asset pricing (see Jarrow [2018]), there exists an equivalent probability measure \mathbb{Q} with respect to \mathbb{P} such that the cryptocurrency price process S is a \mathbb{Q} -local martingale. “Equivalent” means that the probability measures agree on zero probability events in \mathcal{F} , and a local-martingale is a generalization of a martingale. It is called “local”, because the price process behaves like a martingale when stopped on a sequence of stopping times approaching T . \mathbb{Q} is also referred to as a risk-neutral probability measure.

We do not assume that the market is complete, in which case there could be an infinite number of local-martingale measures. If incomplete, we assume that a unique \mathbb{Q} is chosen by the market, either via an economic equilibrium or via the market we are studying being embedded in a larger market that is complete. See Jarrow [2018] and Jarrow et al. [2010].

2.2 The Fundamental Value

We define the fundamental value of the cryptocurrency to be the expected discounted liquidation value of the currency at time T using the risk-neutral probability \mathbb{Q} . More formally, the cryptocurrency’s fundamental value is

$$S_t^{FV} = E_{\mathbb{Q}}[S_T | \mathcal{F}_t].$$

²More formally, we assume that the market satisfies No Free Lunch with Vanishing Risk (NFLVR). See Jarrow [2018] for the definition of NFLVR.

Use of the risk neutral probabilities adjusts for risk in computing this present value. If a trader finds no additional value in re-trading, then her optimal selling time is the final date T . Hence, the fundamental value of the cryptocurrency can be interpreted as its buy and hold value.

2.3 Type 3 Bubbles

An asset's type 3 price bubble is defined to be the difference between the asset's market price and its fundamental value:

$$\beta_t = S_t - S_t^{FV}.$$

This is the standard definition of a price bubble used in the economics literature.

It is now easy to see that a price bubble exists if and only if the asset's price is a *strict* local martingale under the risk neutral probability \mathbb{Q} . Indeed, if the price process is a martingale, then $S_t = E_{\mathbb{Q}}[S_T|\mathcal{F}_t]$ and $\beta_t = 0$. Useful in understanding a price bubble are some of its properties, which follow directly from the definition (see [Jarrow \[2018\]](#)).

1. For all $t \in [0, T]$, $\beta_t \geq 0$.
2. $\beta_T = 0$.
3. If $\beta_s = 0$ for some $s \in [0, T]$, $\beta_t = 0$ for all $t > s$.

Expression (1) states that negative bubbles do not exist, (2) asserts that any existing bubble must burst by the final date, T , and (3) implies that once a bubble collapses, it cannot be reborn.

2.4 The Testing Methodology

In this section, we specify the price evolution of the cryptocurrency and provide a necessary and sufficient condition for it to exhibit a price bubble.

2.4.1 The Cryptocurrency's Price Process

We assume that the cryptocurrency's price is a solution to the following stochastic differential equation under \mathbb{P} :

$$dS_t = \sigma(S_t)dW_t + \mu(S_t, Y_t)dt \quad \text{with } S_0 = 1 \quad (1)$$

$$dY_t = s(Y_t)dC_t + g(Y_t)dt \quad \text{with } Y_0 = 1 \quad (2)$$

where W_t and C_t are independent standard Brownian motions, and Y_t in (2) is additional randomness present in the asset's drift process which results in an incomplete market if μ is not the constant function in Y_t . Note that the cryptocurrency's volatility is a function of the level of the cryptocurrency. It is this dependence that enables us to capture the existence of price bubbles.

Under the risk neutral probability \mathbb{Q} , the evolution for the cryptocurrency is (see [Protter \[2013\]](#))

$$dS_t = \sigma(S_t)dW_t \quad \text{with } S_0 = 1. \quad (3)$$

There is no drift, because the price is normalized by the mma.

2.4.2 The Bubble Test

The following result is the basis for the bubble test. Given in [Mijatović and Urusov \[2012\]](#) and [Delbaen and Shirakawa \[2002\]](#), it states that the price process S given in expression (3) is a strict local martingale under \mathbb{Q} if and only if

$$\int_{\varepsilon}^{\infty} \frac{s}{\sigma(s)^2} ds < \infty \quad \text{for any } \varepsilon > 0. \quad (4)$$

Hence, testing for a price bubble is equivalent to investigating whether the integral in (4) is finite or not. If the integral converges, there is a bubble.

If it diverges, then there is no bubble. Note that this integral is finite if the variance function increases at a faster rate than the price implying the bubbles are associated with large return variances at high price levels. This is the condition underlying our statistical methodology.

3 The Empirical Methodology

In this section, we decompose the empirical detection of cryptocurrency bubbles into two steps:

1. **Estimating the Volatility Function.** We use a non-parametric procedure to obtain the cryptocurrency's volatility and price pairs, $(\hat{\sigma}(S), S)$, given the observed price data over our observation interval.
2. **Interpolation, Extrapolation, and Evaluation Modified Convex Hull Algorithm (MCHA).**
 - (a) *Interpolation:* Form the upper and lower convex hulls of the estimated volatility and price pairs.
 - (b) *Extrapolation:* Follow the **Modified Convex Hull Algorithm (MCHA)** to fit a function to the upper and lower convex hulls.
 - (c) *Evaluation (Point Estimation and Hypothesis Testing):* Using the bubble test criterion (4), determine if the integral under these functions are finite (bubble) or infinite (no bubble) at the 95 percent confidence level.

Next, we provide a brief description and diagnostics of the data. The details of above steps (2a) - (2b) are explained in the volatility estimation section. Finally, we elaborate the interpolation, extrapolation, and evaluation steps of the algorithm.

3.1 Data

This subsection consists of two parts. In the first part, we describe the name, source, period, and basic information of the data we collect and employ for the estimation. In the second part, we present the descriptive statistics of the data.

3.1.1 Source

We collect hourly closing prices of eight cryptocurrencies from the Bloomberg Terminal. The sample period is from January 1, 2019 to July 17, 2019.

Table 1: An Excerpt from the Hourly Price Data

	Bitcoin	Ethereum	Litecoin	Bitcoin Cash	EOS	Monero	Ripple	Zcash
1/2/2019 2:00	3796.49	144.495	31.8	163.47	2.6911	49.345	0.3587	59.869
1/2/2019 3:00	3802.75	145.6	32.281	164.91	2.714	49.252	0.3613	60.468
1/2/2019 4:00	3795.17	145.262	32.045	162.01	2.7023	48.847	0.3601	60.4
1/2/2019 5:00	3807.56	149.08	32.305	162.95	2.7296	49.809	0.3622	61.182
1/2/2019 6:00	3808.98	148.452	32.32	163.1	2.7407	49.603	0.3644	61.243
1/2/2019 7:00	3812.7	148.632	32.24	163.39	2.7362	49.947	0.3637	60.961
1/2/2019 8:00	3842.48	152.465	32.54	165.35	2.7739	50.918	0.3669	61.739

Table 1 is an excerpt from the data set consisting of hourly prices. It comprises time series data for eight cryptocurrencies where the date-stamp ranges from 2 am to 8 am on January 2, 2019. The time zone is Eastern Standard Time. Each price entry in the table represents how much one unit of cryptocurrency X is worth in US Dollars.

The currencies are selected from the top 50 market capitalized cryptocurrencies as of July, 2019. There is a total of 3,466 price observations for each cryptocurrency. Each currency’s volatility estimation is based on its own time series. See 3.2 for the details on the estimation technique.

3.1.2 Description

The descriptive statistics for the eight cryptocurrencies are in the following table.

Table 2: The Descriptive Statistics

	Mean	Skewness	Kurtosis	Std Dev	Min	Max
BTC	5982.84	0.94	2.64	2706.89	3354.56	13843.09
ETH	182.33	0.70	2.09	64.04	101.22	353.42
XRP	0.35	0.85	2.50	0.05	0.28	0.49
LTC	74.01	0.37	1.95	33.15	29.88	142.60
BCH	256.86	0.25	1.48	122.60	107.10	513.41
EOS	4.60	0.17	1.92	1.58	2.22	8.34
XMR	67.11	0.54	2.04	19.85	42.11	119.24
ZEC	68.01	1.02	2.95	17.97	45.94	120.30

Table 2 reports the descriptive statistics of the eight cryptocurrencies in the data set from January 1, 2019 to July 17, 2019 with a total of 3,466 observations.

Skewness represents the degree of asymmetry in the data distribution. The eight cryptocurrencies exhibit some degree of positive skewness with light tailed distributions.

Figure 1: Data Diagnostics on Bitcoin
(Date: 1/1/2019-11/17/2019)

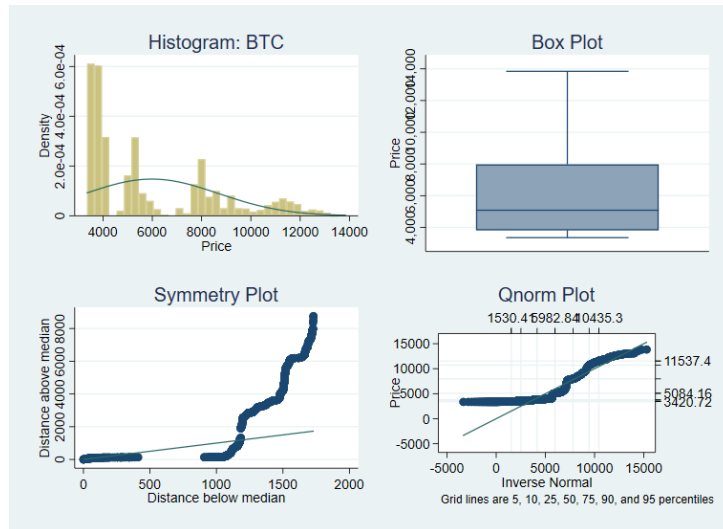


Figure 1 illustrates the four diagnostics we perform on the Bitcoin price series: histogram, box, symmetry, and q-norm plots.

In addition, we perform four diagnostics to visually examine each cryptocurrency series for any anomaly in the data set. Nothing unusual was discovered, and the diagnostic plots for all currencies are in the Appendix C.

3.2 Volatility Estimation

In this subsection, we perform the non-parametric estimation developed by Florens-Zmirou [1993] to estimate the volatility function. Jarrow et al. [2011a] use this technique to investigate the presence of a bubble in LinkedIn's stock price following its IPO, and Chaim and Laurini [2019] employ this method to estimate Bitcoin's price volatility.

3.2.1 The Florens-Zmirou Estimator

Consider a simpler version of the stochastic differential equation (1):

$$dS_t = \sigma(S_t)dW_t + \mu(S_t)dt \quad \text{with } S_0 = 1, t \in [0, T] \quad (5)$$

The objective is to estimate the diffusion coefficient, $\sigma(S_t)$. Florens-Zmirou [1993] constructs a consistent estimator for $\sigma(S_t)$ based on the local time of this diffusion process. The local time characterizes the amount of time a particle spends at a level or in an interval. Florens-Zmirou [1993]'s estimator of $\sigma(x)^2$ for a sample of size n is:

$$\hat{\sigma}_n(x)^2 = \frac{\sum_{i=1}^{n-1} 1_{\{|S_{t_i} - x| < h_n\}} n(S_{t_{i+1}} - S_{t_i})^2}{\sum_{i=1}^n 1_{\{|S_{t_i} - x| < h_n\}}} \quad (6)$$

where h_n represents a positive real sequence converging to zero as $n \rightarrow \infty$. Taking the square root of expression (6) yields our estimate of the volatility function $\sigma(x)$.

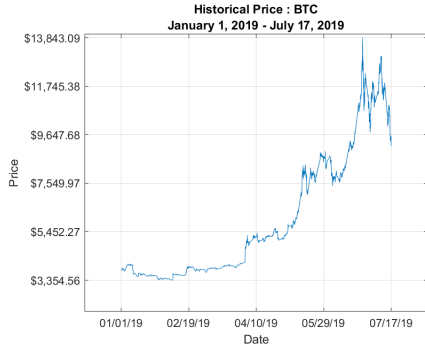
Given a finite horizon $[0, T]$, the technique employs regular sampling following a partition of $t_i = \frac{T}{n}$ for $i = 1, \dots, n$. For confidence intervals,

a useful convergence theorem states that if nh_n^3 converges to zero, then $\sqrt{\sum_{i=1}^n 1_{\{|S_{t_i}-x|<h_n\}}} \left(\frac{\hat{\sigma}_n(x)^2}{\sigma(x)^2} - 1 \right)$ converges to $\sqrt{2}Z$ where Z is the standard normal variable (see [Florens-Zmirou \[1993\]](#), Theorem 1, p. 800 for details).

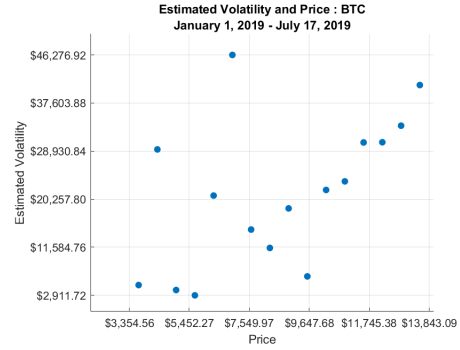
3.2.2 Estimation Results

This section provides the non-parametric estimation results for eight cryptocurrencies from January 1, 2019 to July 17, 2019. The original data set comprises a total of 3,466 hourly price observations for each cryptocurrency. Expressions (1) and (2) correspond to a local stochastic volatility model. Over a short time interval (e.g. our sample period), it can be viewed as an approximation to a more complex stochastic volatility model. Performing our estimation over this short time interval is consistent with the economics underlying type 3 bubbles, which result from speculative trading over a finite horizon. To illustrate the procedure, we first explore the Bitcoin's estimated volatility and price pairs.

Figure 2: Bitcoin's Historical Price and Estimated Volatility
(Date: 1/1/2019-7/17/2019)



(a) Bitcoin **Hourly** Price



(b) Estimated Volatility for Bitcoin

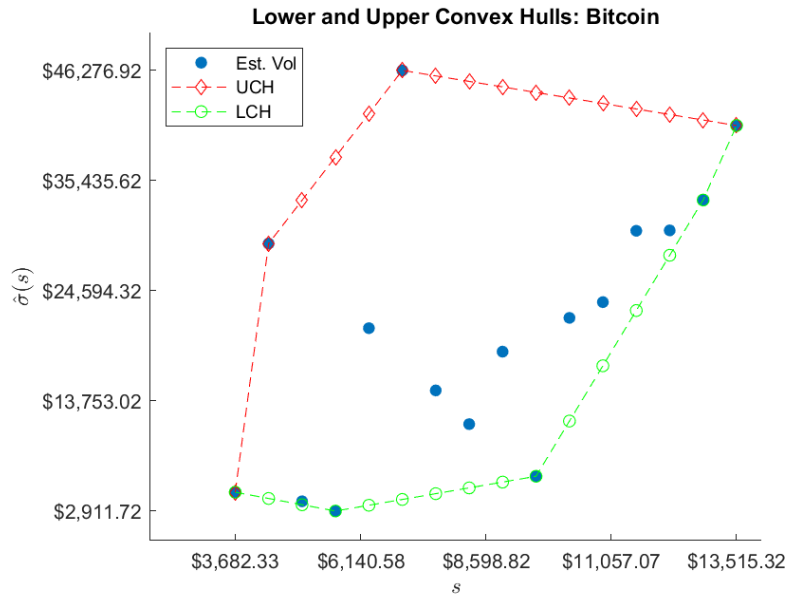
Figure (2a) displays the historical price of Bitcoin with approximately 3,400 observations. As depicted, Bitcoin's price process exhibited exponential growth, such growth is often associated with alleged price bubbles. Figure (2b) represents Bitcoin's price and volatility pairs. Here, the volatility

appears to increase with the price level at an increasing pace. Appendix D contains the figures for the volatility and price pairs for all of the remaining seven cryptocurrencies.

3.3 Interpolation

We introduce a new technique called the **Modified Convex Hull Algorithm (MCHA)** that simplifies the interpolation and extrapolation steps while enhancing its robustness. The algorithm focuses on computing the integral in expression (4) using various upper and lower approximations to determine if it is finite or infinite. This approach is distinct from Jarrow et al. [2011a]. For clarity, the reason for fitting upper and lower bounds for the volatility function instead of using a single approximating function across price and volatility pairs is discussed after our methodology is presented (see section 3.5).

Figure 3: Bitcoin's Modified Convex Hull
(Date: 1/1/2019-11/17/2019)



We illustrate the approach with Bitcoin again. Consider the price and estimated volatility pairs for Bitcoin computed from the observations between January 1, 2019 and July 17, 2019. In Figure (3), the blue dots are the estimated volatility points. The green and red dashed lines represent the lower and upper convex hulls for these set of points, respectively. The green circles on the lower convex hull represent the projections of the price and volatility pairs on the lower convex hull. Similarly for the red circles on the upper convex hull. We denote the new set of estimated volatility points on the lower convex hull as LCH^B , B for Bitcoin. Similarly, we produce the set of new estimated volatility points on the upper convex hull and denote them as UCH^B (See the Appendix A and E for details on the exact computations).

3.4 Extrapolation and Evaluation

In this section, we explain the methodology which consists of (i) extrapolating the modified convex hulls constructed from the interpolation step, (ii) computing point estimates of a parameter in order to evaluate the integrals of these extrapolated volatility functions, and (iii) performing a hypothesis test, controlling for both Type 1 and Type 2 errors.

1. *Extrapolation* : We select the best power functions $f(x) = \alpha x^\beta$ to fit the lower and upper convex hulls. We linearize the approximating functions as

$$\ln(\sigma) = \ln(\alpha) + \beta \ln(S) + \varepsilon \quad (7)$$

and perform ordinary least squares (OLS) to obtain the estimated coefficients $\hat{\beta}$ for the best fitting approximations to the lower and upper convex hulls.

2. *Evaluation (Point Estimation)*:

- (a) We first compute a point estimate of β in order to evaluate the *upper bound* for the integral in expression (4). The upper bound is

evaluated using the *lower*³ convex hull's approximating function to see if it converges. For the power function, if the estimated coefficient $\hat{\beta}_u > 1$, then this point estimate implies the integral in expression (4) converges.

- (b) If the point estimate of β implies the lower convex hull integral diverges, then this does not guarantee divergence of the true integral. In this case we use the *upper* convex hull to compute a point estimate of the *lower bound* for the integral in expression (4).
- (c) If the point estimate of β implies that the upper convex hull integral diverges, then because it is a lower bound for the true integral, the true integral itself diverges, and there is no bubble. For the power function, if $\hat{\beta}_l \leq 1$, then this point estimate implies the integral in expression (4) diverges, and there is a no bubble.
- (d) If the point estimate of β implies the upper bound integral converges, then the test is inconclusive. For the power function this occurs if $\hat{\beta}_l > 1$.

3. *Evaluation (Hypothesis Testing)*: This section discusses how to perform hypothesis testing using the point estimate of β obtained in the previous section. Since we are computing point estimates of β in order to evaluate the lower and upper bounds on the integral, the following algorithm controls for both Type 1 and Type 2 errors.

- (a) Step 1: Test the null hypothesis of “No Bubble” using the point estimate of β to evaluate the upper bound on the true integral at the 0.95 confidence level. For the power function, reject the null if $\hat{\beta}_u > 1 + 1.645\hat{\sigma}_u$. See [Hypothesis Testing](#) in Appendix for the justification of this critical region. If rejected, stop. The conclusion is that a bubble exists. Otherwise due to the fact that

³The reversal of the upper convex hull and a lower approximation to the integral is due to the fact that the volatility is in the denominator, for details see the Appendix A.

this is upper bound and there is potentially a large Type 2 error, go to step 2.⁴

- (b) Step 2: Test the null hypothesis of “Bubble” using the point estimate of β to evaluate the lower bound on the true integral at the 0.95 confidence level. For the power function, reject the null if $\hat{\beta}_l \leq 1 - 1.645\hat{\sigma}_l$. If rejected, stop. The conclusion is that there is no bubble.
- (c) Step 3: Stop. The testing is inconclusive, because step 1 accepts the hypothesis of no bubble and step 2 accepts the hypothesis of a bubble, both tests having potentially large Type 2 errors.

Table 3: The Bubble Test at 95% Confidence Level via the **Modified Convex Hull Algorithm (MCHA)**

Bound on Integral	Null Hypothesis	Conclusion
No Bubble		
Step 1: Upper	Reject if $\hat{\beta}_u > 1 + 1.645\hat{\sigma}_u$	Bubble
	if $\hat{\beta}_u \leq 1 + 1.645\hat{\sigma}_u$	Go to Step 2
Bubble		
Step 2: Lower	Reject if $\hat{\beta}_l \leq 1 - 1.645\hat{\sigma}_l$	No Bubble
	if $\hat{\beta}_l > 1 - 1.645\hat{\sigma}_l$	Go to Step 3
Step 3: Stop	Accept Both Nulls	Inconclusive

Table 3 summarizes the decision rule (also see Appendix A, **Modified Convex Hull Algorithm (MCHA)**). The lower and upper convex hull integrals, as characterized by the power function’s β exponent, provide sufficient conditions for the absence and presence of bubbles.

⁴The explanation for why the Type 2 error in Step 1 is controlled for in Step 2 is as follows. In Step 1, the Type 2 error is $\mathbb{P}(\text{Accept No-Bubble}|\text{No-Bubble False})$. To see that the Type 2 error is potentially large, suppose that $\beta = 1 + \varepsilon$ for ε small, then this probability is nearly 0.95. Note that in Step 2, the Type 1 error is $0.05 = \mathbb{P}(\text{Reject Bubble}|\text{Bubble True}) = \mathbb{P}(\text{Accept No-Bubble}|\text{Bubble True}) = \mathbb{P}(\text{Accept No-Bubble}|\text{No-Bubble False})$ which is the Type 2 error in Step 1.

We illustrate this procedure with Bitcoin. Figure 4 provides the fit of the power function to Bitcoin’s estimated volatility and price sets for its lower convex hull. From Figure 4, we observe that the 95% confidence bandwidth is fairly tight.

Figure 4: Estimation on Lower Convex Hull: Bitcoin
(Date: 1/1/2019-7/17/2019)

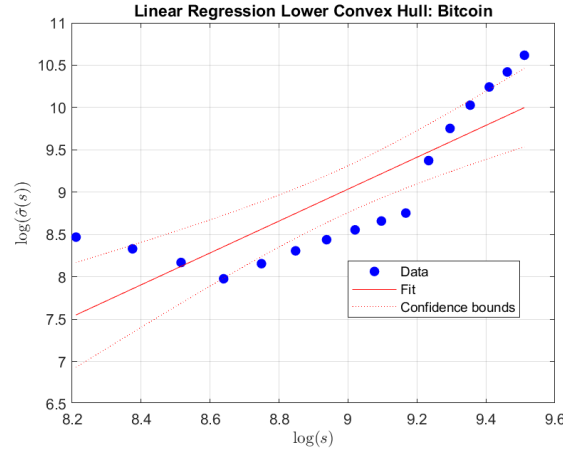


Table 4 contains the regression estimates. As indicated, the power function provides a good fit to the lower convex hull with a large R^2 and a small standard error for $\hat{\beta}_u$.

Table 4: Estimation Results for Bitcoin
Upper Bound on Integral

Currency	$\hat{\alpha}_u$	SE	$\hat{\beta}_u$	SE	95% CR	R^2
BTC*	-7.920	2.987	1.884	0.332	1.5446	69.69%

Applying the decision rule, the case of Bitcoin concludes in Step 1. We see that Bitcoin’s estimated $\hat{\beta}_u = 1.884 > 1 + 1.645(.332) = 1.5446$, which implies that the null hypothesis of no bubble is rejected at the 95 percent confidence level. For Bitcoin, there is no reason to consider the upper convex hull.

3.5 Discussion

This section uses the Bitcoin example to explain the reason for fitting upper and lower bounds for the volatility function instead of using a single approximating function across the price and volatility pairs. Figure 5 gives the graph of the best fitting power function to Bitcoin's price and estimated volatility pairs and Table 5 contains the regression estimates.

From an economic point of view, fitting the best power function to Bitcoin's price and estimated volatility pairs implies that we are assuming the evolution of price process is given by a constant elasticity of variance (CEV) process, i.e.

$$dS_t = \alpha S_t^\beta dW_t + \mu(S_t)dt \quad \text{with } S_0 = 1. \quad (8)$$

As seen in Figure 5 and Table 5, a CEV process provides a very poor fit to the cryptocurrency's evolution. Indeed, the R^2 is quite low (32.8%) and the standard error of the estimated β is quite large (0.477). Using this evolution to determine whether Bitcoin has a bubble or not is problematic, because the CEV process provides a poor fit to the currency's true evolution.

Figure 5: CEV Regression on Estimated Vol & Price Set
(Bitcoin, Date: 1/1/2019-7/17/2019)

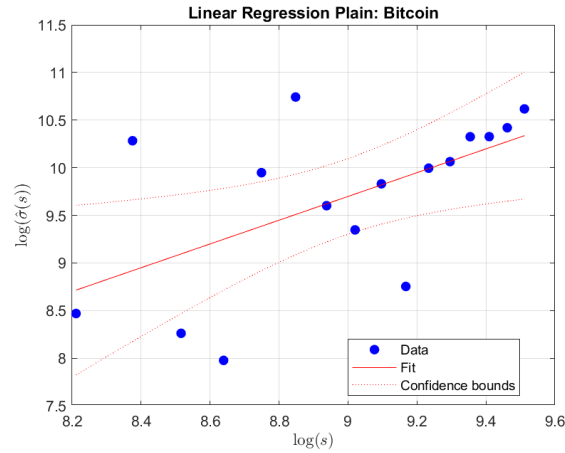


Table 5: Estimation Results for Bitcoin using CEV Process

Currency	$\hat{\alpha}$	SE	$\hat{\beta}$	SE	R^2
CEV	-1.530	4.294	1.248	0.477	32.80%

In contrast, by using the MCHA algorithm (fitting the lower and upper convex hulls), we do not assume a particular evolution for the cryptocurrency (i.e. we do not determine the exact functional form of $\sigma(S_t)$). Instead, we bound the “true” function with power functions from above and below. The novelty of our technique stems from using these approximating functions to determine whether the integral of the true volatility function converges or diverges. The consistency of our methodology with an arbitrary volatility function is a strength of the **Modified Convex Hull Algorithm (MCHA)**.

4 Results

In this section, we provide the results from applying the **Modified Convex Hull Algorithm (MCHA)** to determine if bubbles exists in each of the eight cryptocurrencies. The cryptocurrencies are: Bitcoin (BTC), Litecoin (LTC), Ethereum (ETH), Ripple (XRP), Bitcoin Cash (BCH), EOS (EOS), Monero (XMR), and Zcash (ZEC). Of these cryptocurrencies, all except ETH and EOS are general payment tokens, which serve as a medium of exchange. Both ETH and EOS are platform tokens, which serve a dual role by providing other services or functions as well. See [Cong et al. \[2020b\]](#). We illustrated these computations with Bitcoin in the previous section. The complete set of regression results is in Appendix **K**.

The following table summarizes the estimation results produced from fitting a power function to the lower convex hull for the cryptocurrencies from January 1, 2019 to July 17, 2019.

Using the MCHA algorithm and as documented in Table **6**, Bitcoin (BTC), Ripple (XRP), Bitcoin Cash (BCH), EOS (EOS), Monero (XMR),

Table 6: Hypothesis Testing of No Bubble
(Upper Bound on Integral (4))

Currency	$\hat{\alpha}_u$	SE	$\hat{\beta}_u$	SE	95% CR	R^2
BTC*	-7.920	2.987	1.884	0.332	1.5446	69.69%
LTC	3.627	0.711	0.143	0.162	1.2665	5.32%
ETH	-0.420	0.865	1.058	0.161	1.2731	75.57%
XRP*	0.582	0.034	1.932	0.035	1.0576	99.55%
BCH*	-1.117	0.661	1.238	0.117	1.1925	88.95%
EOS*	-1.137	0.320	1.795	0.195	1.3208	85.84%
XMR*	-2.192	1.024	1.523	0.235	1.3866	75.01%
ZEC*	-4.184	0.305	1.944	0.069	1.1135	98.25%

and Zcash (ZEC) all reject the null hypothesis of no bubble at the 95% confidence level. Hence, these currencies exhibit a bubble. For LTC and ETH, the null hypothesis of no bubble cannot be rejected. Hence, for these currencies, we need to examine the upper convex hull approximations to obtain a lower bound to the integral.

Figure 6 demonstrates the convex hulls for Ethereum and Litecoin. The estimation results from fitting the power function to Litecoin's and Ethereum's upper convex hulls are provided in Table 7.

Figure 6: Ethereum and Litecoin's Convex Hulls
(Date: 1/1/2019-7/17/2019)

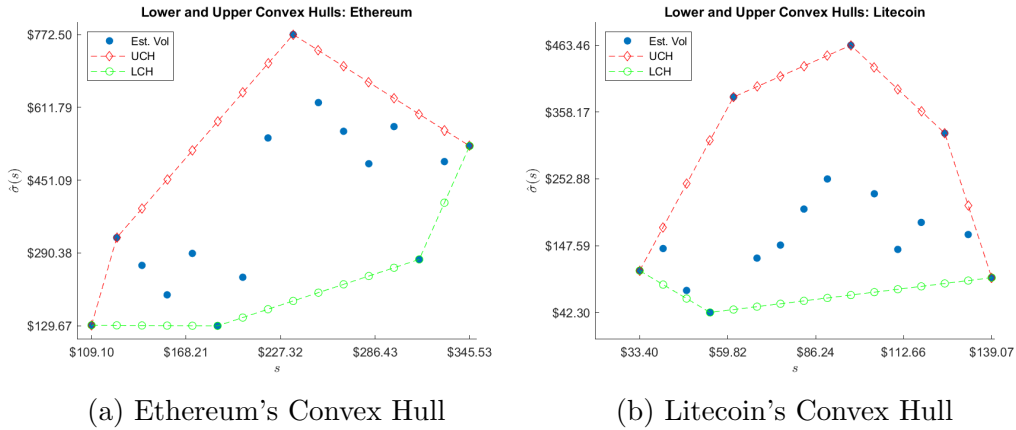


Table 7: Hypothesis Testing of Bubble
(Lower Bound on Integral (4))

Currency	$\hat{\alpha}_l$	SE	$\hat{\beta}_l$	SE	95% CR	R^2
LTC*	4.404	1.291	0.293	0.294	0.5163	6.65%
ETH	1.450	1.200	0.895	0.223	0.6332	53.53%

It provides the hypothesis tests for the alternative null hypothesis of a bubble. For Litecoin (LTC), the cut-off rejects the hypothesis of a bubble. Consequently, LTC exhibits no price bubble. For Ethereum (ETH), the cut-off does not reject the null hypothesis of a bubble. Hence, the test is inconclusive for ETH because both null hypotheses are accepted.

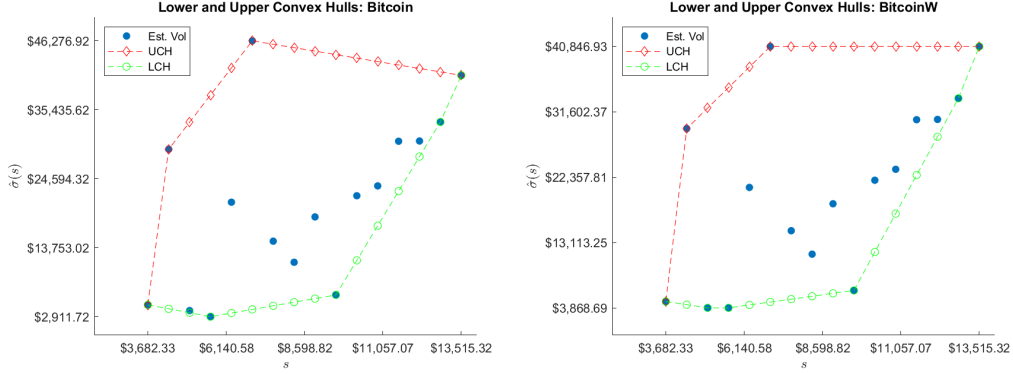
5 Robustness Tests

This section provides two robustness tests of our bubble testing methodology.

5.1 Outlier Analysis

The first robustness test can be interpreted as an outlier analysis. Given that our volatility estimates contain error, it is important to test the robustness of the convex hulls created by the **Modified Convex Hull Algorithm (MCHA)**. When estimating the price and volatility pairs, the largest and smallest volatility estimates in the sample are the most likely to contain the largest error component. These price and volatility pairs may affect the convex hull construction more than proportionate to their percentage in the sample. To control for this possibility, we winsorize the data by replacing the maximum and minimum estimated volatility points with their respective second max and min points. This type of filter is standard in statistics when examining the robustness of the empirical model with respect to outliers. Then, we repeat our hypothesis testing procedure.

Figure 7: Bitcoin's Convex Hulls After Winsorizing Max & Min Points
(Date: 1/1/2019-7/17/2019)



(a) Bitcoin's Original Convex Hull

(b) Bitcoin's Convex Hull Post-Filter

In Figure 7, we illustrate the post-filter convex hulls for Bitcoin. See Appendix L for the complete set of winsorized convex hulls.

In Table 8, we provide the regression results using winsorization.

Table 8: Hypothesis Test of No Bubble
Post Winsorization: Cryptocurrencies
(Upper Bound on Integral (4))

Currency	$\hat{\alpha}_u$	SE	$\hat{\beta}_u$	SE	95% CR	R^2
BTC*	-6.973	2.751	1.785	0.306	1.503	70.89%
LTC	4.326	0.250	0.034	0.057	1.093	2.49%
ETH	-0.398	0.855	1.055	0.159	1.261	75.87%
XRP	-0.718	0.005	0.193	0.005	1.008	99.09%
BCH*	-1.108	0.663	1.237	0.117	1.192	88.88%
EOS*	-0.378	0.159	1.395	0.097	1.159	93.68%
XMR*	-1.427	0.821	1.368	0.188	1.310	79.02%
ZEC*	-2.890	0.310	1.661	0.071	1.116	97.54%

Following our decision rule in Table 3, we conclude that BTC, BCH, EOS, XMR, and ZEC exhibit bubbles. For LTC, ETH, and XRP, we proceed to the decision rule's Step 2 and investigate the regression results using the upper convex hulls.

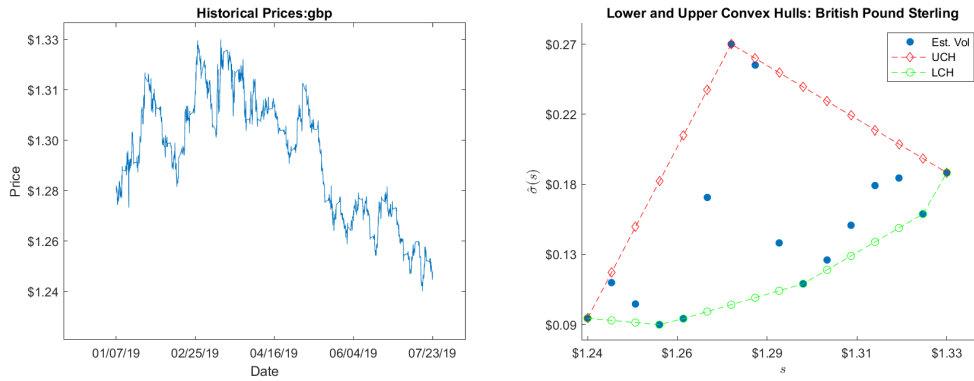
Table 9: Hypothesis Test of Bubble
Post Winsorization: Cryptocurrencies
(Lower Bound on Integral (4))

Currency	$\hat{\alpha}_l$	SE	$\hat{\beta}_l$	SE	95% CR	R^2
LTC*	4.580	1.190	0.240	0.271	0.555	5.32%
ETH	1.542	0.973	0.859	0.181	0.703	61.70%
XRP	0.452	0.423	0.767	0.433	0.288	18.35%

LTC exhibits no bubble while the evidence for bubbles in both ETH and XRP are inconclusive. See Appendix L for the full regression results of the winsorized convex hulls for the cryptocurrencies. As documented, our conclusion is adjusted for only one cryptocurrency XRP. After winsorization, the evidence is inconclusive with respect to XRP exhibiting a bubble or not.

5.2 Foreign Exchange Rates

Figure 8: USD-GBP's Historical Exchange Rate & Estimated Volatility
(Date: 1/7/2019-7/23/2019)



(a) USD-GBP **Hourly** Exchange Rates (b) Estimated Volatility (USD-GBP)

As a second robustness test of the MCHA algorithm, we apply it to more standard foreign currencies: US Dollars (USD) to Japanese Yen (JPY), Great British Pound (GBP), Canadian Dollar (CAD), and Euro (EUR) over a

similar time period January 7, 2019 to July 23, 2019 using hourly exchange rates. The purpose of which is to discover whether the methodology provides similar or dissimilar results.

For illustration, Figure 8 displays the USD-GBP historical exchange rates and its estimated volatility and prices accompanied with the lower and upper convex hulls.⁵ The estimation results for all four currencies are provided in Table 10. The Great British Pound (GBP), the Canadian Dollar (CAD), and the Euro (EUR) reject the null hypothesis of no bubble at the 0.95 confidence level, implying that these currencies exhibit a bubble.

Table 10: Hypothesis Test of No Bubbles for the
Foreign Currencies
(Upper Bound on Integral (4))

Currency	$\hat{\alpha}_u$	SE	$\hat{\beta}_u$	SE	95% CR	R^2
JPY	-11.378	23.938	-0.817	5.097	9.385	0.18%
GBP*	-4.630	0.208	9.822	0.823	2.353	91.06%
CAD*	-2.289	0.005	3.928	0.016	1.026	99.98%
EUR*	-3.285	0.007	1.893	0.053	1.087	98.93%

For the Japanese Yen (JPY), we cannot reject the null hypothesis of no bubble. Using the MCHA algorithm, we proceed to fit the power function on the JPY's upper convex hull.

Figure 9 illustrates the historical prices of Japanese Yen (JYP) in US Dollars with the corresponding convex hull. Table 11 provides the estimation results. For the JPY, the upper bound test rejects the null hypothesis of a bubble. Hence, there is no bubble for the JPY.

Just as for cryptocurrencies, three of the four currencies tested herein exhibit price bubbles over the same time period. The evidence suggests that these standard foreign currencies are not dissimilar to cryptocurrencies in this regard and that they are also held for speculative purposes and not just

⁵Each exchange rate indicates how much a unit of the foreign currency is worth in US Dollars (e.g. 1 Canadian Dollar equals .76 US Dollars).

for their use as a medium of exchange.

Figure 9: JPY Historical Price & Upper Convex Hull
(Date: 1/7/2019-7/23/2019)

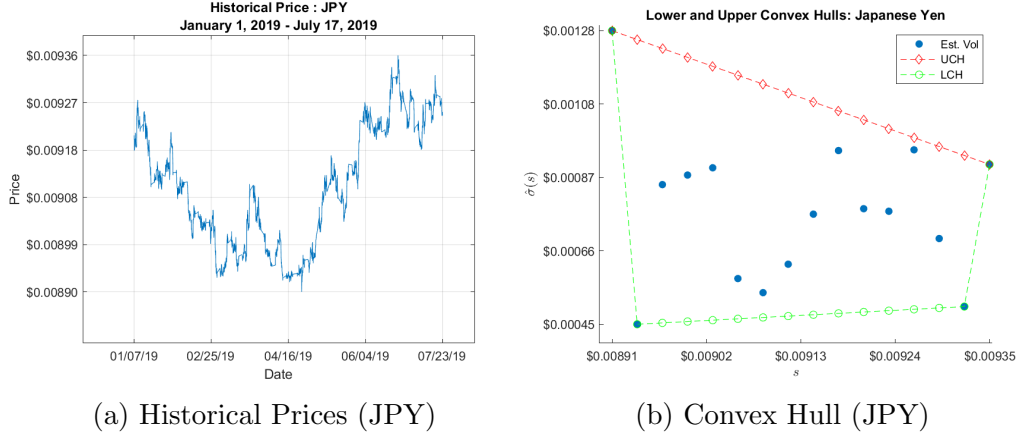


Table 11: Hypothesis Testing of Bubble for the
USD to Japanese Yen
(Lower Bound on Integral (4))

Currency	$\hat{\alpha}_l$	SE	$\hat{\beta}_l$	SE	95% CR	R^2
JPY*	-41.348	0.500	-7.352	0.1064	0.8250	99.71%

Finally, we apply the winsorized version of the MCHA to examine the robustness of our model for the standard currencies.

Table 12: Hypothesis Test of No Bubbles for the
Foreign Currencies (Winsorized)
(Upper Bound on Integral (4))

Currency	α_u	SE	β_u	SE	95% CR	R^2
JPY	-9.276	17.403	-0.375	3.7056	7.0958	0.07%
GBP*	-4.556	0.209	9.549	0.8293	2.3642	90.45%
CAD	-3.332	0.000	0.000	0.0000	1.0000	100.00%
EUR	-3.033	0.010	0.131	0.0759	1.1249	17.45%

Following the decision rule in Table 6, our analysis yields that GBP exhibit a bubble while we cannot reject the null of no bubble for JPY, CAD, and EUR.⁶ Table 12 provides the results.

We proceed with the upper convex hull of these currencies to test the null hypothesis of a bubble. Table 13 rejects the null hypothesis of a bubble in the JPY.

Table 13: Hypothesis Testing of Bubble for the
JPY, CAD, EUR (Winsorized)
(Lower Bound on Integral (4))

Currency	α_u	SE	β_u	SE	95% CR	R^2
JPY*	-9.608	0.839	-0.562	0.1786	0.7920	41.45%
CAD	-0.712	1.797	7.077	6.3209	-6.3607	8.22%
EUR	-4.197	1.021	15.367	8.0508	-8.3752	20.65%

The evidence is inconclusive for both the CAD and the EUR. This robustness test further supports the validity of the local martingale theory of bubbles, and it provides strong evidence for the theory’s applicability to a wide range of asset classes.

6 Conclusion

This paper contributes to the literature concerning asset price bubbles in several ways. First, examining the presence of bubbles in cryptocurrencies has enabled us to test the feasibility of applying the local martingale theory of bubbles in its most natural experimental setting. The cryptocurrency market is known for its short-term speculation-driven momentum, which perfectly corresponds to the local martingale theory’s investigation of the *type 3* bubbles. In addition, the absence of cash flows in the cryptocurrency market further supports the laboratory setting. We find the prevalence of bubbles

⁶Note the Canadian dollar rates produce a zero slope with its winsorized lower convex hull which is a horizontal line.

in the major cryptocurrencies. Hence, the paper strongly supports the local martingale theory of bubbles, and the theory easily extends to popular asset classes such as equities, fixed income, and foreign currencies.

Although a few empirical methodologies to test the local martingale theory of bubbles have been proposed, our paper creates a novel algorithm called the **Modified Convex Hull Algorithm (MCHA)** to test for the presence of bubbles. The algorithm is simple to use and it revolves around the convergence of an integral expression defined over the entire positive real line (4) using upper and lower bounds. We introduce hypothesis testing of this convergence, controlling for Type I and especially large Type II errors.

We show that the **Modified Convex Hull Algorithm (MCHA)** is robust by performing an outlier analysis that winsorizes the maximum and minimum estimated volatility and price pairs. Winsorization yields almost identical results with the exception of one cryptocurrency, XRP, which changes from a bubble to being inconclusive. Moreover, we apply our testing methodology to four standard foreign currencies. The British Pound exhibits a bubble while a bubble does not exist in the Japanese Yen. The evidence for both the Canadian Dollar and the Euro is inconclusive. Applying our procedure to foreign currencies reinforces the theory's wide applicability to multiple asset classes.

Finally, our findings provide a cautionary note for policymakers considering the integration of cryptocurrencies into the market. As both public and private sectors continue to make aggressive moves to do so, their daily use as a medium of exchange seems inappropriate given the pervasiveness of bubbles in these currencies.

References

- Elie Bouri, Rangan Gupta, and David Roubaud. Herding behaviour in cryptocurrencies. *Finance Research Letters*, 29:216 – 221, 2019.
- Markus K. Brunnermeier and Martin Oehmke. Chapter 18 - bubbles, financial crises, and systemic risk. volume 2 of *Handbook of the Economics of Finance*, pages 1221 – 1288. Elsevier, 2013.
- Pedro Chaim and Márcio P. Laurini. Is bitcoin a bubble? *Physica A: Statistical Mechanics and its Applications*, 517:222 – 232, 2019.
- Eng-Tuck Cheah and John Fry. Speculative bubbles in bitcoin markets? an empirical investigation into the fundamental value of bitcoin. *Economics Letters*, 130:32 – 36, 2015.
- Lin Cong, Xi Li, Ke Tang, and Yang Yang. Crypto wash trading. *Working Paper, Cornell University*, 2020a.
- Lin Cong, Ye Li, and Neng Wang. Token-based platform finance. *SSRN Working Paper*, 2020b.
- Freddy Delbaen and Hiroshi Shirakawa. No arbitrage condition for positive diffusion price processes. *Asia-Pacific Financial Markets*, 9:159–168, 2002.
- Danielle Florens-Zmirou. On estimating the diffusion coefficient from discrete observations. *Journal of Applied Probability*, 30(4):790–804, 1993. ISSN 00219002.

- Julian Geuder, Harald Kinateder, and Niklas F. Wagner. Cryptocurrencies as financial bubbles: The case of bitcoin. *Finance Research Letters*, 31:179–184, 2019.
- John Griffin and Amin Shams. Is bitcoin really un-tethered? *The Journal of Finance*, *Forthcoming*, 2019.
- Robert Jarrow. *Continuous-Time Asset Pricing Theory*. Springer International Publishing, first edition, 2018.
- Robert Jarrow, Younes Kchia, and Philip Protter. Is there a bubble in linkedin’s stock price? *The Journal of Portfolio Management*, 38(1):125–130, 2011a.
- Robert Jarrow, Younes Kchia, and Phillip Protter. How to detect an asset bubble. *SIAM Journal on Financial Mathematics*, 2(1):839–865, 2011b.
- Robert A. Jarrow, Philip Protter, and Kazuhiro Shimbo. Asset price bubbles in incomplete markets*. *Mathematical Finance*, 20(2):145–185, 2010.
- Tao Li, Donghwa Shin, and Baolian Wang. Cryptocurrency pump-and-dump schemes. *Working Paper*, 2019.
- Aleksandar Mijatović and Mikhail Urusov. On the martingale property of certain local martingales. *Probability Theory and Related Fields*, 152:1–30, 2012.
- Philip Protter. *Stochastic Integration and Differential Equation*. Springer-Verlag, Berlin, Heidelberg, second edition, 2005.

Philip Protter. A mathematical theory of financial bubbles. *Paris-Princeton Lectures on Mathematical Finance 2013*, 11(1):1–108, 2013.

Appendices

A Modified Convex Hull Algorithm (MCHA)

The non-parametric estimation yields a set of estimated volatility and price pairs based on the range of prices visited by the cryptocurrency process. To compute the integral in expression (4), we need a technique to interpolate and extrapolate the estimated volatility and price pairs. We developed the Modified Convex Hull Algorithm (MCHA) for this purpose. This new algorithm uses an upper and lower approximation for the volatility function to compute bounds on the integral. We now describe the algorithm for the general case.

1. Let $S = \{\text{the set of estimated price and volatility pairs } (x, \hat{\sigma}(x))\}$.
2. Denote the upper and lower convex hull of S as $Conv_U(S)$ and $Conv_L(S)$, respectively.
3. To compute the lower convex hull, consider the estimated ordered pair of volatility and prices:
 $\{(\hat{\sigma}_1, S_1), (\hat{\sigma}_2, S_2), \dots, (\hat{\sigma}_N, S_N)\}$, ordered by prices $S_1 < S_2 < \dots < S_N$.
4. Follow this **iterative process** to calculate the *Modified Convex Hulls*:
 - (a) Let S_i represents the crypto-currency's i^{th} price in the set.
 - (b) Start with the lowest price and estimated volatility pair: $(S_1, \hat{\sigma}_1)$. We denote this as the **Reference Point (RP)**.
 - (c) Perform this iterative process⁷: compute the angle from the RP to each of other points $i \in \{2, \dots, N\}$.

$$\theta_{RP,i} = \arctan \left(\frac{\hat{\sigma}_i - \hat{\sigma}_{RP}}{S_i - S_{RP}} \right) \quad (9)$$

⁷Note $-90 < \theta_{RP,i} < 90$ otherwise the iteration has issues or the estimated points must be revisited.

- (d) Compute the minimum (maximum) angle in degrees for the next lower (upper) convex hull forming point.
- (e) Identify the index of the angle to which the RP has the minimum degree.
- (f) Update the **RP** and repeat the steps from (b) to (e) until you reach $i = N$.
- (g) When we are done with step (f), we have the set of points that forms the lower and upper convex hull for each currency.
- (h) Next we move onto projecting the remaining estimated points onto the convex hull lines.
- (i) Consider *lower convex hull* for illustration.
- (j) For notation purposes, denote the lower convex hull forming point points to be:

$$LCH = \{S_1, S_4, S_{15}, S_{16}\}. \quad (10)$$

- (k) Compute the parameters for the linear equation between each subsequent points in LCH . For instance, if you have k elements in LCH , then you will have $k - 1$ linear equations connecting the k points. Project the remaining points above onto these lines between the forming points. This produces the new set of estimated volatility values, $\hat{\sigma}_i$ for all $i = 1, \dots, N$.
- (l) We denote the set of the newly computed estimated volatility and price pairs as

$$LCH = \{(S_i, \hat{\sigma}_i) : i = 1, \dots, N\}. \quad (11)$$

- (m) Repeat the steps from (h) to (l) for the Upper Convex Hull.

5. Computing approximations to the integral $\int_{\varepsilon}^{\infty} \frac{s}{\sigma(s)^2} ds$.

- (a) Let $\sigma_L(s), \sigma(s), \sigma_U(s)$, be the lower convex hull approximation, the actual, and the upper convex hull approximation for the volatility function, respectively. Note that

$$\sigma_L(s)^2 \leq \sigma(s)^2 \leq \sigma_U(s)^2. \quad (12)$$

Thus, the inequalities reverse with respect to the ratios yield

$$\frac{s}{\sigma_L(s)^2} \geq \frac{s}{\sigma(s)^2} \geq \frac{s}{\sigma_U(s)^2}. \quad (13)$$

Hence, the corresponding integrals produce

$$\int_{\varepsilon}^{\infty} \frac{s}{\sigma_L(s)^2} ds \geq \int_{\varepsilon}^{\infty} \frac{s}{\sigma(s)^2} ds \geq \int_{\varepsilon}^{\infty} \frac{s}{\sigma_U(s)^2} ds. \quad (14)$$

(b) **The Algorithm and (Deterministic) Decision Rule:**

- i. Compute the upper bound to the integral using the modified lower convex hull (i.e. $\int_{\varepsilon}^{\infty} \frac{s}{\sigma_L(s)^2} ds$):
 - A. If $\int_{\varepsilon}^{\infty} \frac{s}{\sigma_L(s)^2} ds < \infty$, then

$$\int_{\varepsilon}^{\infty} \frac{s}{\sigma(s)^2} ds \leq \int_{\varepsilon}^{\infty} \frac{s}{\sigma_L(s)^2} ds < \infty \quad (15)$$

There exists a bubble.

- B. *Otherwise, it is inconclusive.* Go to 5(b)ii.

- ii. Compute the lower bound to the integral using the modified upper convex hull (i.e. $\int_{\varepsilon}^{\infty} \frac{s}{\sigma_U(s)^2} ds$):
 - A. If $\int_{\varepsilon}^{\infty} \frac{s}{\sigma_U(s)^2} ds = \infty$, then

$$\int_{\varepsilon}^{\infty} \frac{s}{\sigma(s)^2} ds = \infty \leq \int_{\varepsilon}^{\infty} \frac{s}{\sigma_U(s)^2} ds = \infty \quad (16)$$

There is no bubble.

B. *Otherwise, it is inconclusive.* In this case, we have shown,
for some $\int_{\varepsilon}^{\infty} \frac{s}{\sigma_U(s)^2} ds = K \in \mathbb{R}_+$,

$$\int_{\varepsilon}^{\infty} \frac{s}{\sigma_U(s)^2} ds \leq \int_{\varepsilon}^{\infty} \frac{s}{\sigma(s)^2} ds \leq \int_{\varepsilon}^{\infty} \frac{s}{\sigma_L(s)^2} ds \quad (17)$$

$$K \leq \int_{\varepsilon}^{\infty} \frac{s}{\sigma(s)^2} ds \leq \infty \quad (18)$$

In the text, this algorithm is refined in two ways: First, the algorithm is modified to use the power function to approximate the lower and upper bounds on the volatility function, and second, by second the algorithm is modified by adding sampling error and a hypothesis test to the decision rule.

B Hypothesis Testing

Our hypothesis testing is based on the following construct:

$$H_0 : \beta \leq 1 \tag{19}$$

$$H_A : \beta > 1 \tag{20}$$

Let the critical region (reject the null hypothesis) be when $\hat{\beta} \geq K$ for K a constant. Assume $\hat{\beta} = \beta + \sigma\varepsilon$ where $\varepsilon \sim \text{Normal}(0,1)$ with $\sigma > 0$ a constant.

Based on the Central Limit Theorem, this assumption follows approximately from the regression estimation.

The power function for this test is

$$\mathbb{P}(\hat{\beta} \geq K) = \mathbb{P}(\beta + \sigma\varepsilon \geq K) = 1 - N\left(\frac{K - \beta}{\sigma}\right)$$

where $N(\cdot)$ is the cumulative standard normal distribution function.

Given K , first choose the β that solves

$$\sup_{\beta \leq 1} \left[1 - N\left(\frac{K - \beta}{\sigma}\right) \right],$$

yielding the largest possible type 1 error across all possible β consistent with the null hypothesis. The solution is given by $\beta = 1$.

Next, we want to choose K such that the largest type 1 error possible is only 0.05. Hence, at the 0.95 confidence level, solving $1 - N\left(\frac{K-1}{\sigma}\right) = 0.05$ gives this K , i.e. it implies that $K = 1 + \sigma z_{0.95}$ where $N(z_{0.95}) = 0.95$.

C Data Diagnostics

The figures in this section provide the four diagnostics for each cryptocurrency series: histogram, box, symmetry, and q-norm plots.

Figure 10: Data Diagnostics on Bitcoin
(Date: 1/1/2019-11/17/2019)

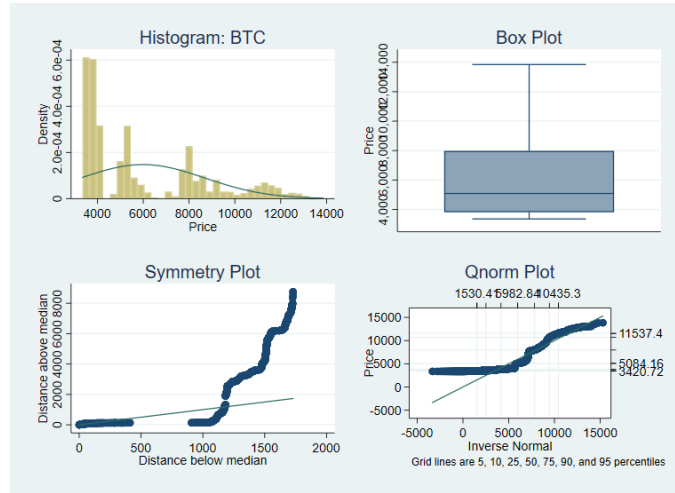


Figure 11: Data Diagnostics on Ethereum
(Date: 1/1/2019-11/17/2019)

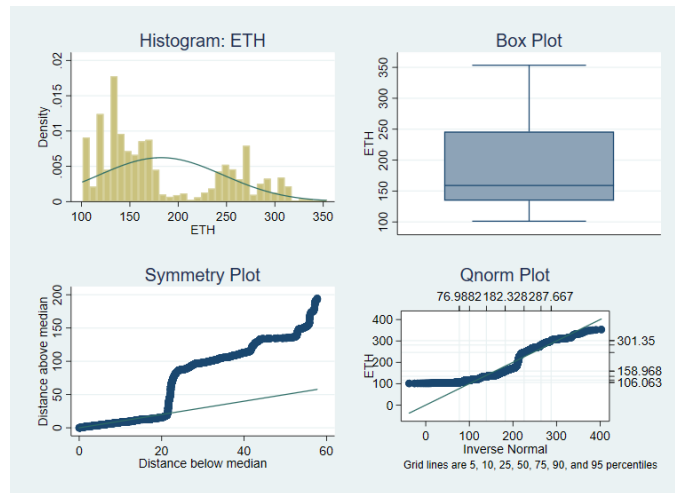


Figure 12: Data Diagnostics on Ripple
(Date: 1/1/2019-11/17/2019)

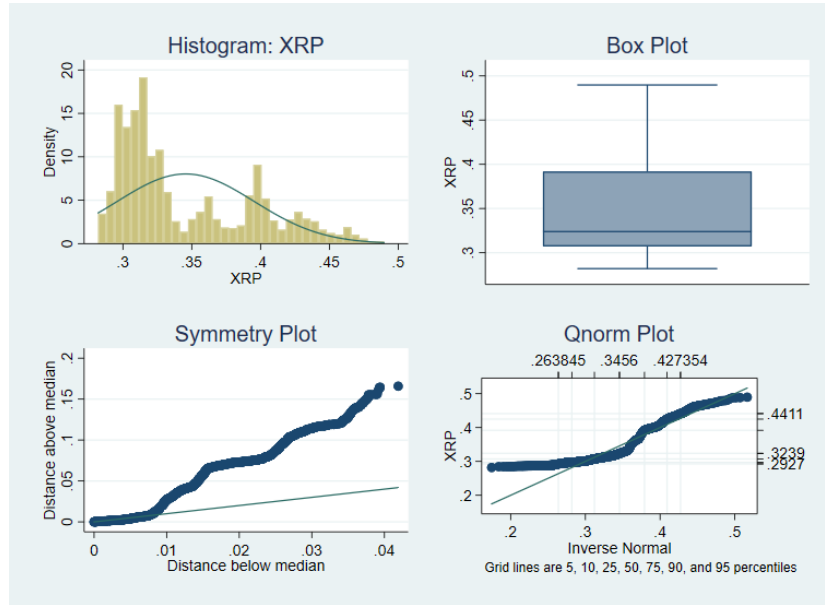


Figure 13: Data Diagnostics on Litecoin
(Date: 1/1/2019-11/17/2019)

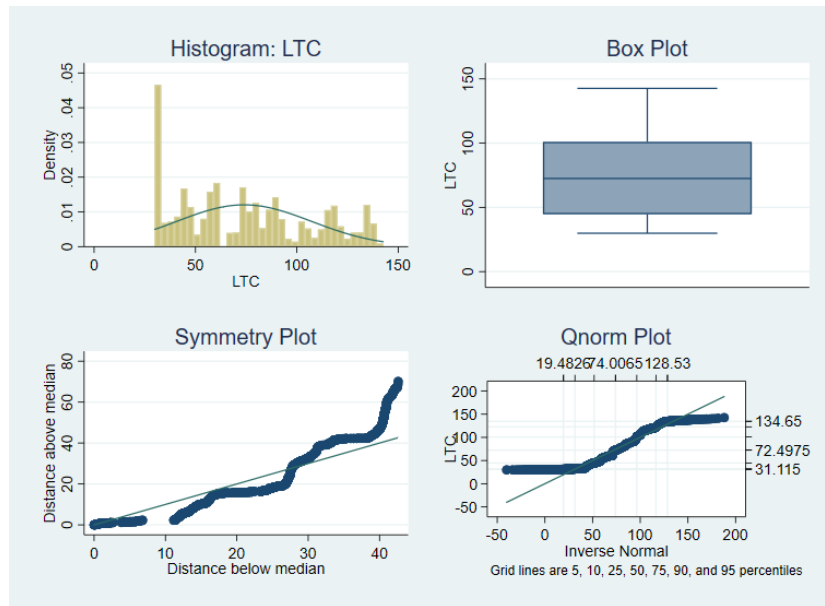


Figure 14: Data Diagnostics on Bitcoin Cash
(Date: 1/1/2019-11/17/2019)

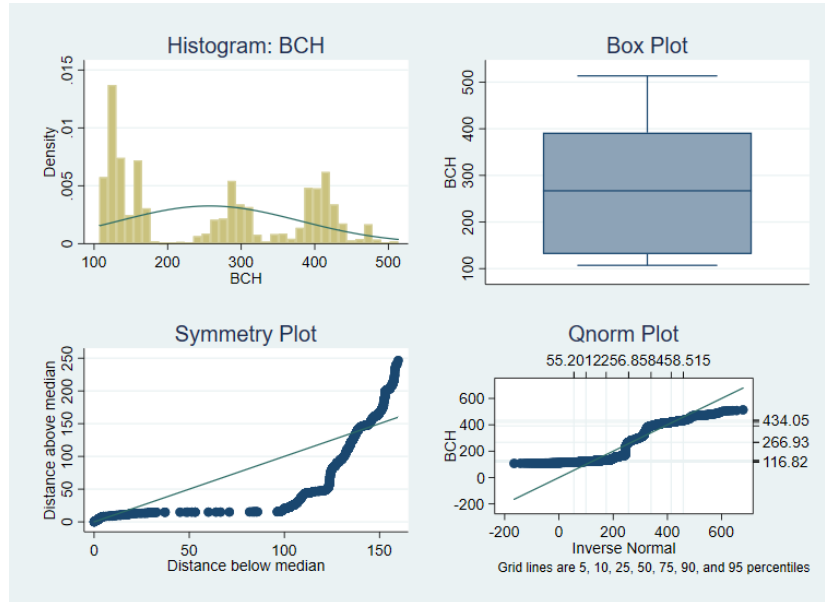


Figure 15: Data Diagnostics on EOS
(Date: 1/1/2019-11/17/2019)

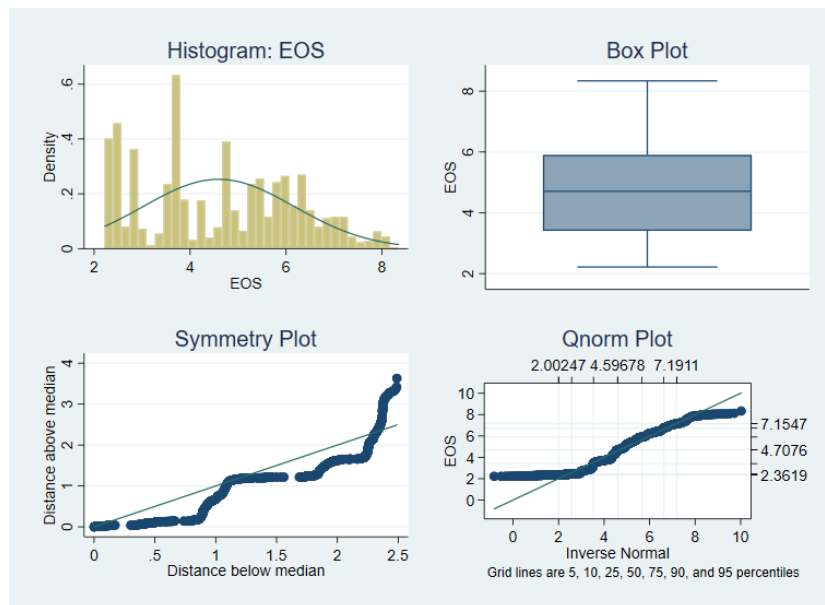


Figure 16: Data Diagnostics on Monero
(Date: 1/1/2019-11/17/2019)

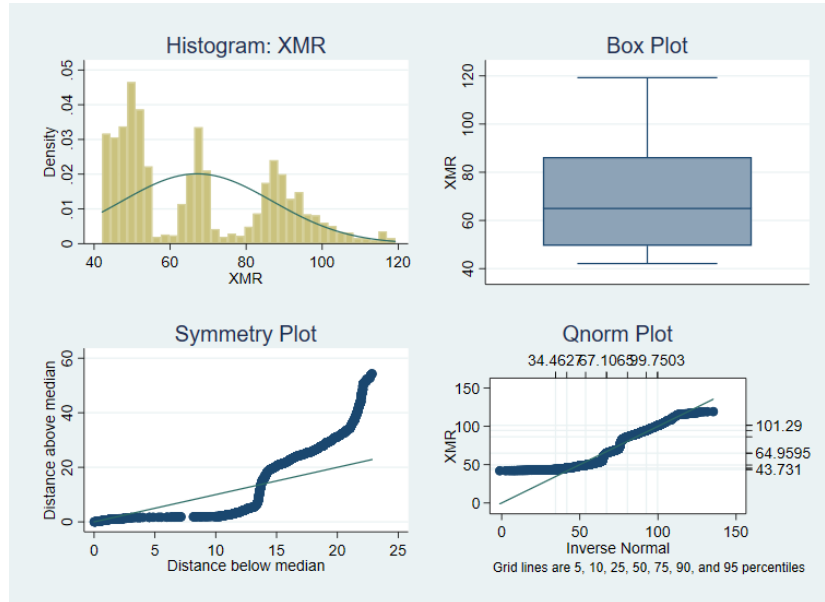
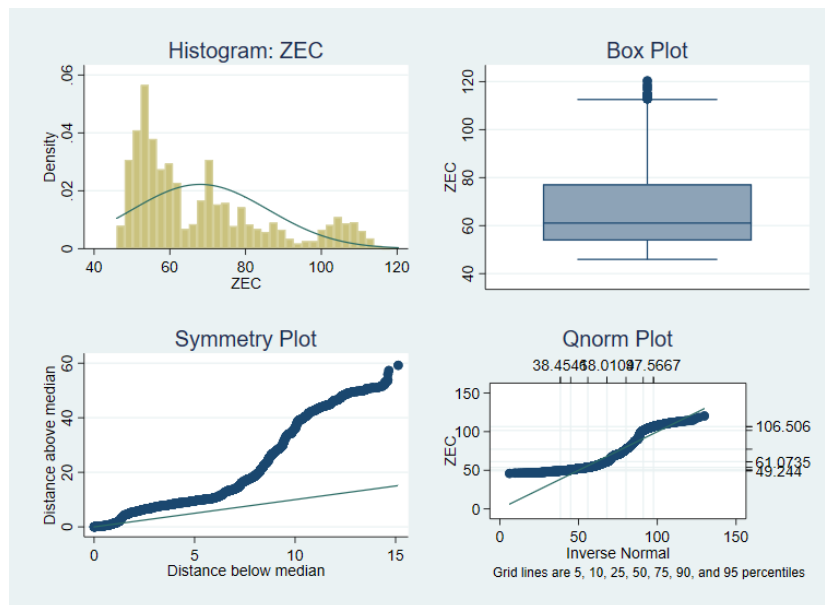


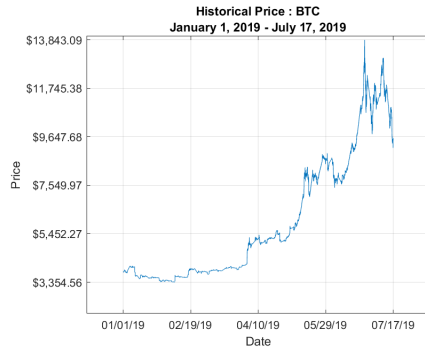
Figure 17: Data Diagnostics on Zcash
(Date: 1/1/2019-11/17/2019)



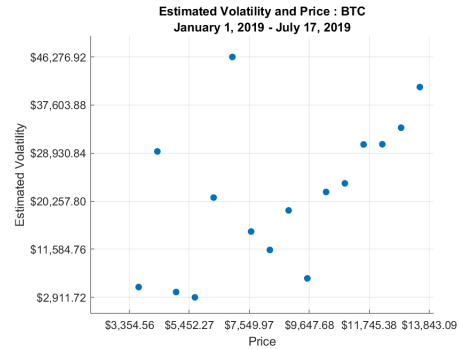
D Volatility Estimation Results

The figures in this section provide the historical prices and estimated volatility for the 8 cryptocurrency. The original data set comprises a total of 3,466 hourly price observations for each cryptocurrency.

Figure 18: Historical Price and Estimated Volatility for Bitcoin, Ethereum, and Ripple



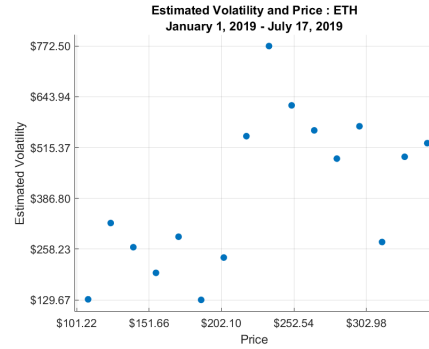
(a) Bitcoin **Hourly** Price



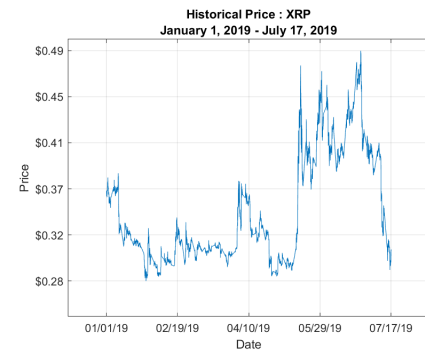
(b) Estimated Volatility for Bitcoin



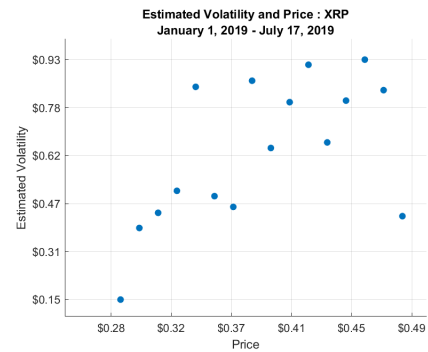
(c) Ethereum **Hourly** Price



(d) Estimated Volatility for Ethereum



(e) Ripple **Hourly** Price

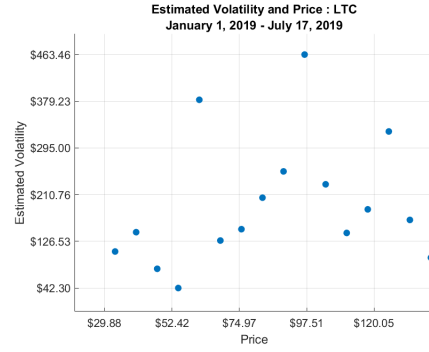


(f) Estimated Volatility for Ripple

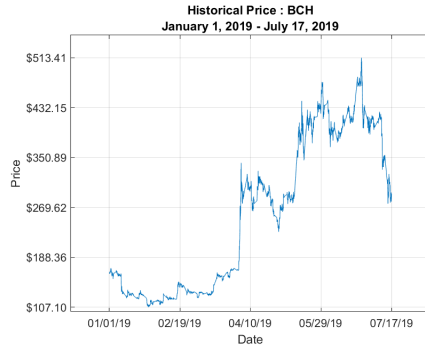
Figure 19: Historical Price and Estimated Volatility for Litecoin, Bitcoin Cash, and EOS



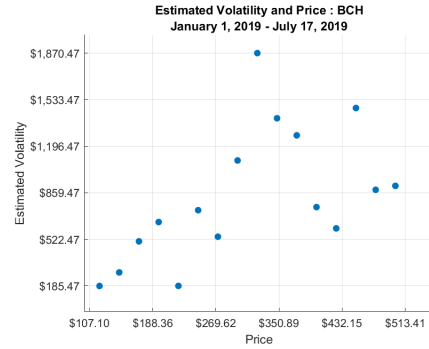
(a) Litecoin **Hourly** Price



(b) Estimated Volatility for Litecoin



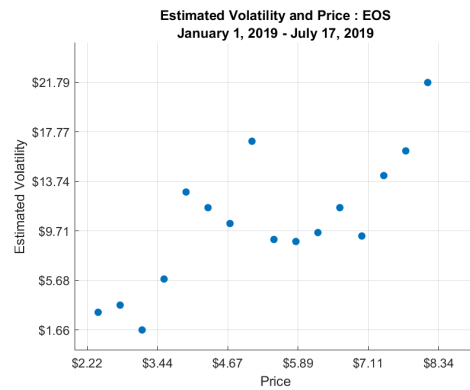
(c) Bitcoin Cash **Hourly** Price



(d) Estimated Volatility for Bitcoin Cash



(e) EOS **Hourly** Price

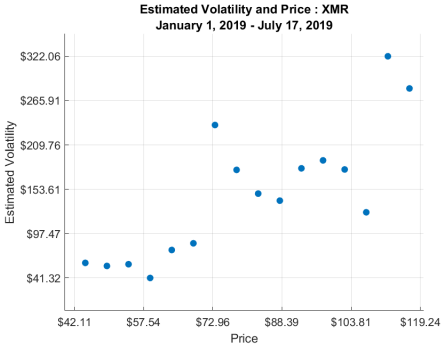


(f) Estimated Volatility for EOS

Figure 20: Historical Price and Estimated Volatility for Monero and ZCash



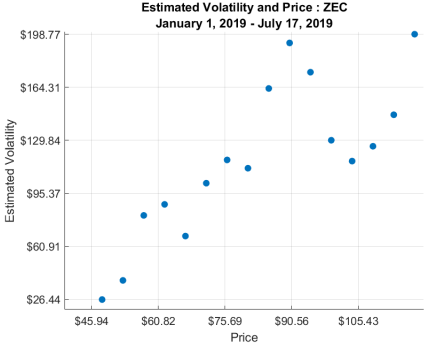
(a) Monero **Hourly** Price



(b) Estimated Volatility for Monero



(c) ZCash **Hourly** Price



(d) Estimated Volatility for ZCash

E Interpolation (Cryptocurrency)

The figures in this section demonstrate how the modified upper and lower convex hulls are constructed for each cryptocurrency. They are constructed with the original estimated volatility and price pairs.

Figure 21: Bitcoin's Modified Convex Hull
(Date: 1/1/2019-7/17/2019)

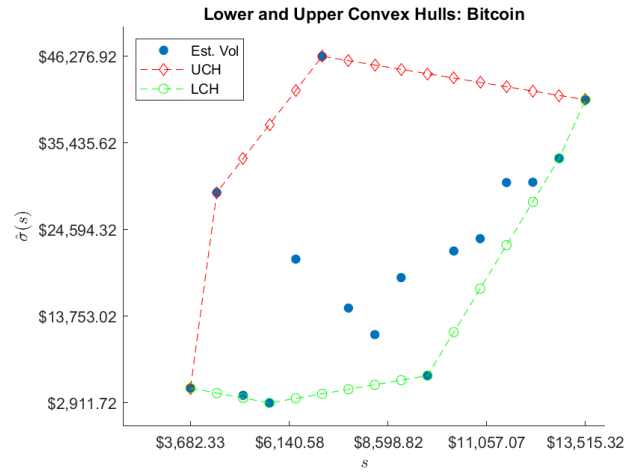


Figure 22: Litecoin's Modified Convex Hull
(Date: 1/1/2019-7/17/2019)

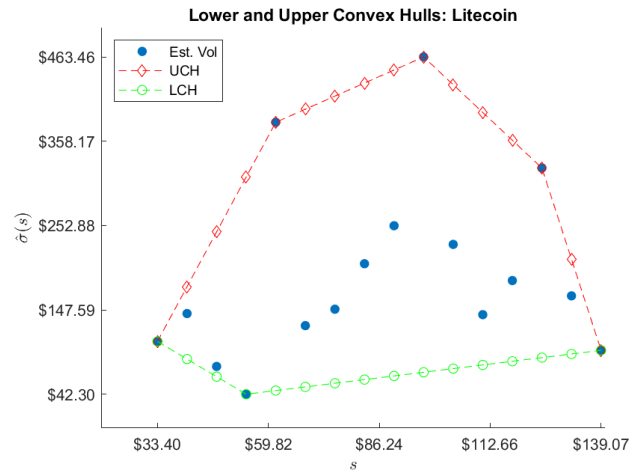


Figure 23: Ethereum's Modified Convex Hull
(Date: 1/1/2019-7/17/2019)

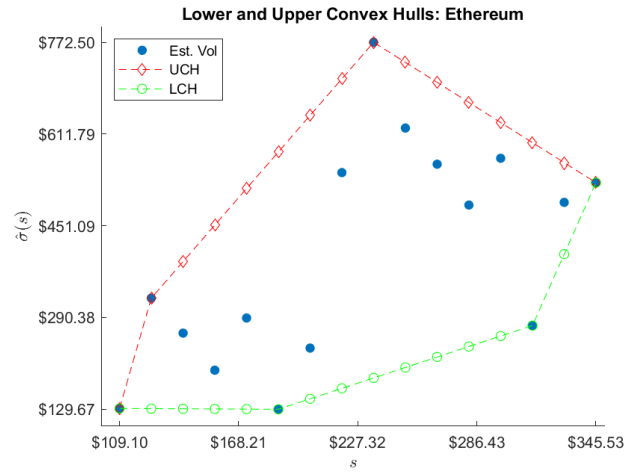


Figure 24: Ripple's Modified Convex Hull
(Date: 1/1/2019-7/17/2019)

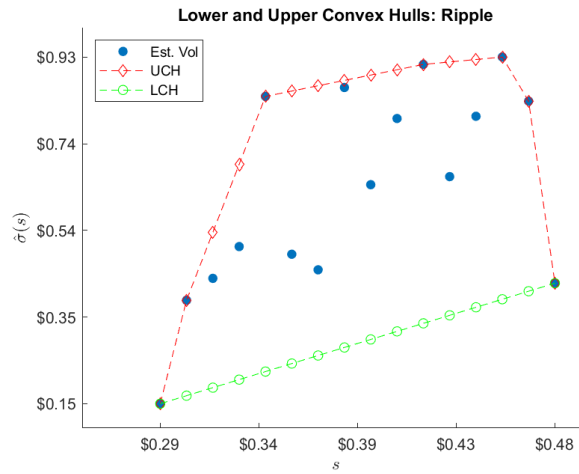


Figure 25: Bitcoin Cash's Modified Convex Hull
(Date: 1/1/2019-7/17/2019)

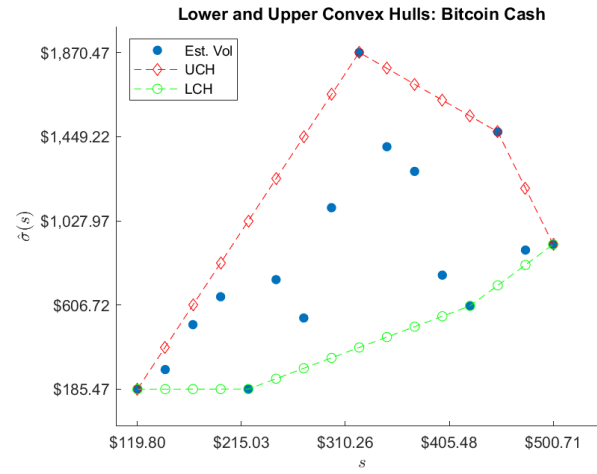


Figure 26: EOS's Modified Convex Hull
(Date: 1/1/2019-7/17/2019)

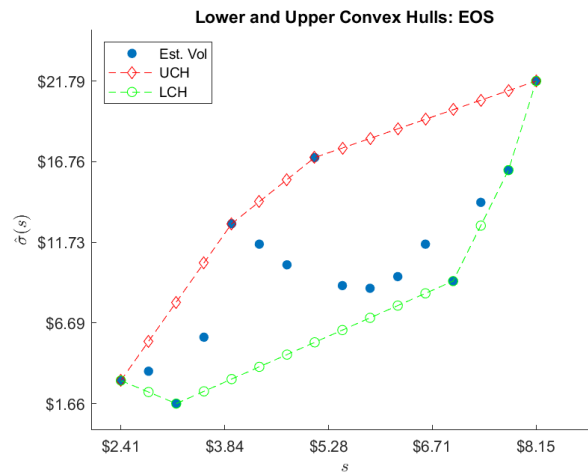


Figure 27: Monero's Modified Convex Hull
(Date: 1/1/2019-7/17/2019)

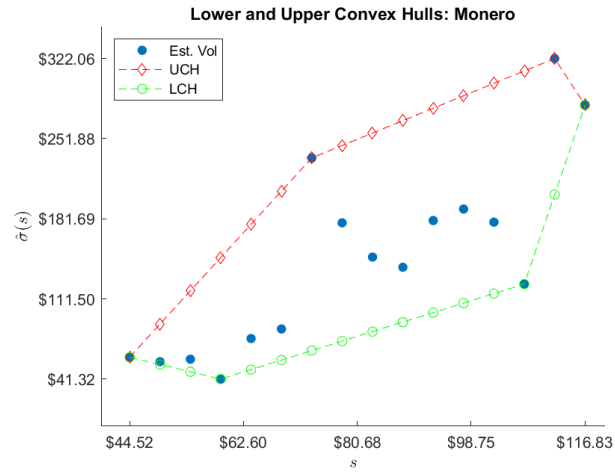
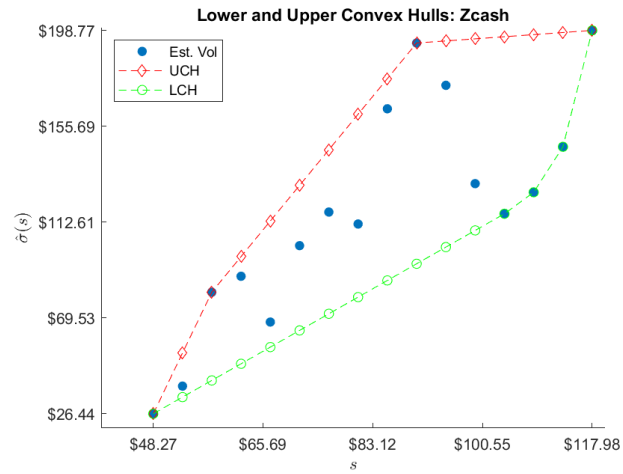


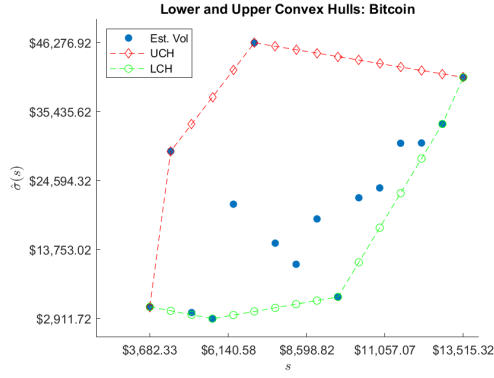
Figure 28: Zcash's Modified Convex Hull
(Date: 1/1/2019-7/17/2019)



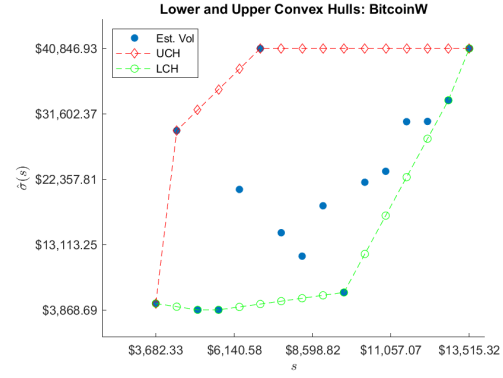
F Interpolation (Crypto, Winsorized)

The figures in this section demonstrate how the modified upper and lower convex hulls are constructed for each cryptocurrency when the maximum and minimum volatility points are replaced with their second highest and lowest points.

Figure 29: Bitcoin's Convex Hulls After Winsorizing Max & Min Points
(Date: 1/1/2019-7/17/2019)

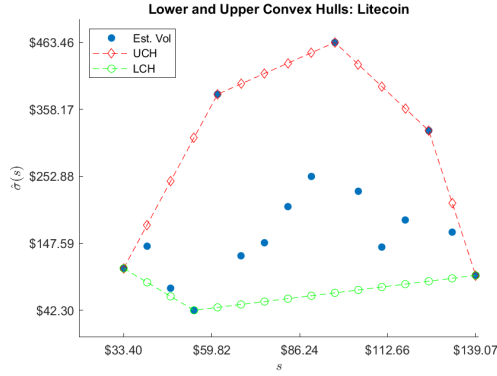


(a) Bitcoin's Original Convex Hull

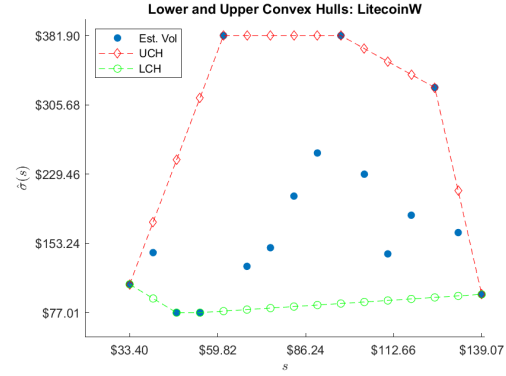


(b) Bitcoin's Convex Hull Post-Filter

Figure 30: Litecoin's Convex Hulls After Winsorizing Max & Min Points
(Date: 1/1/2019-7/17/2019)

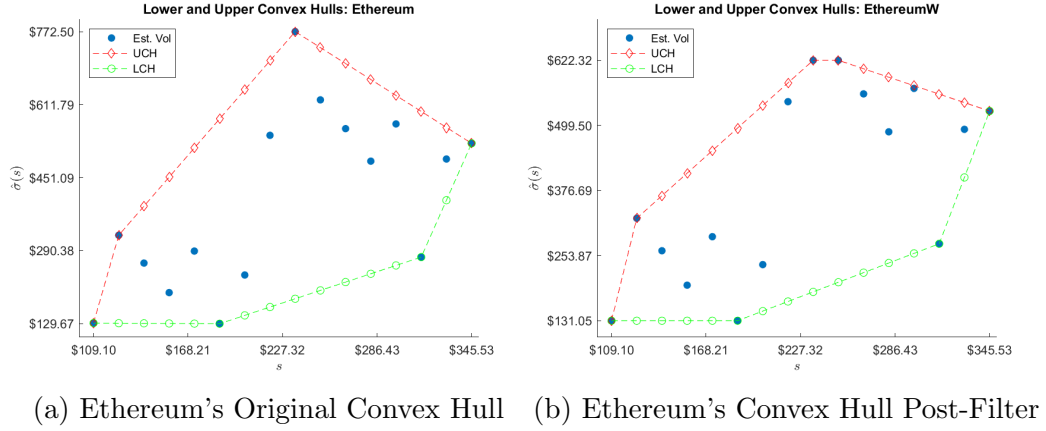


(a) Litecoin's Original Convex Hull



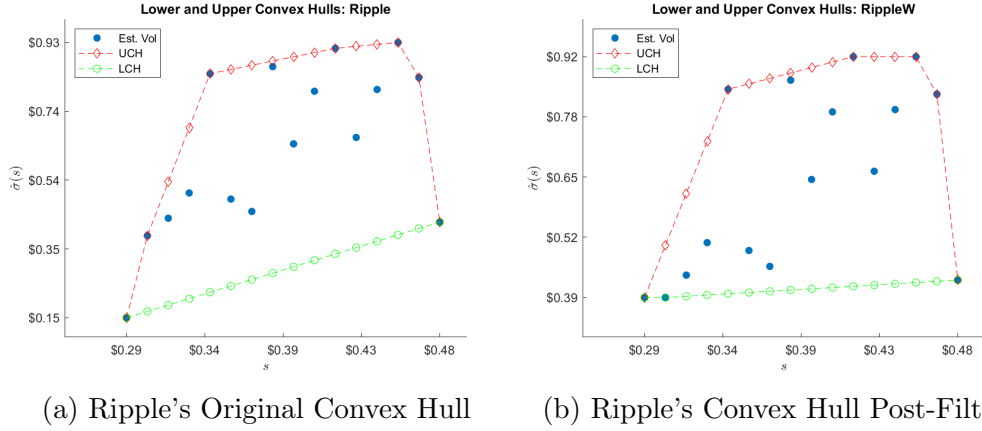
(b) Litecoin's Convex Hull Post-Filter

Figure 31: Ethereum's Convex Hulls After Winsorizing Max & Min Points
(Date: 1/1/2019-7/17/2019)



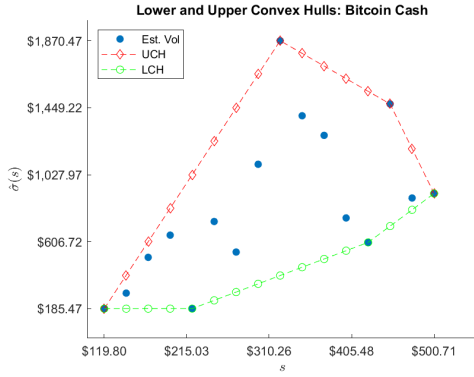
(a) Ethereum's Original Convex Hull (b) Ethereum's Convex Hull Post-Filter

Figure 32: Ripple's Convex Hulls After Winsorizing Max & Min Points
(Date: 1/1/2019-7/17/2019)

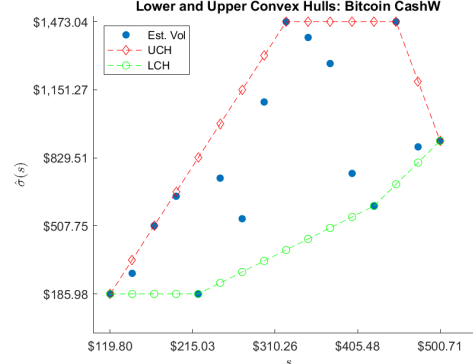


(a) Ripple's Original Convex Hull (b) Ripple's Convex Hull Post-Filter

Figure 33: Bitcoin Cash's Convex Hulls After Winsorizing Max & Min Points
(Date: 1/1/2019-7/17/2019)

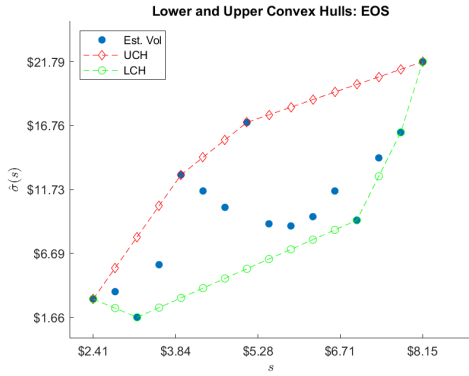


(a) Bitcoin Cash's Original Convex Hull

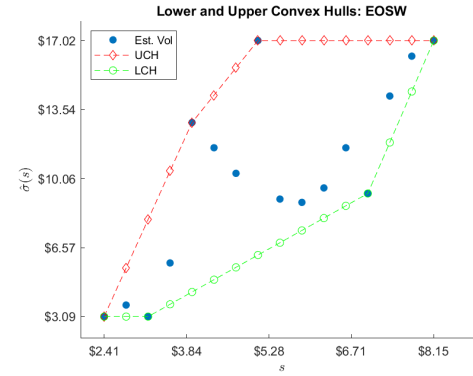


(b) Bitcoin Cash's Convex Hull Post-Filter

Figure 34: EOS's Convex Hulls After Winsorizing Max & Min Points
(Date: 1/1/2019-7/17/2019)

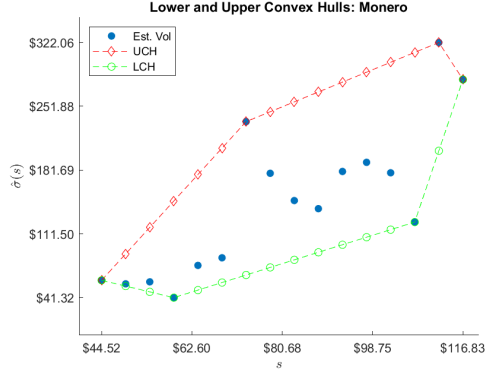


(a) EOS's Original Convex Hull

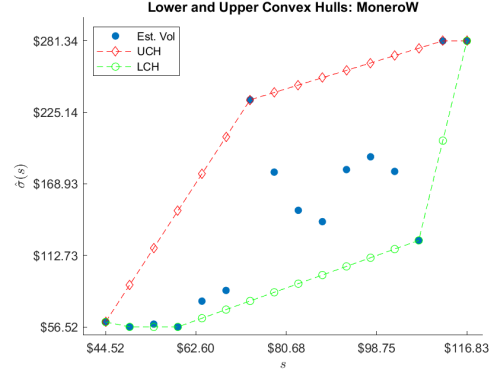


(b) EOS's Convex Hull Post-Filter

Figure 35: Monero's Convex Hulls After Winsorizing Max & Min Points
(Date: 1/1/2019-7/17/2019)

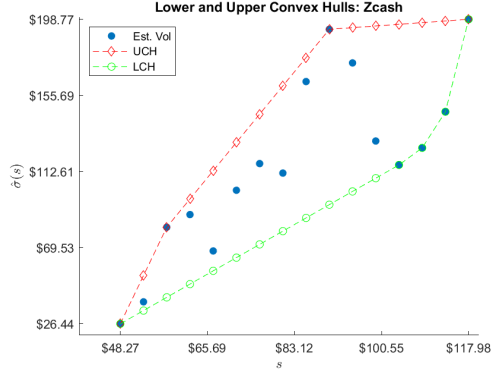


(a) Monero's Original Convex Hull

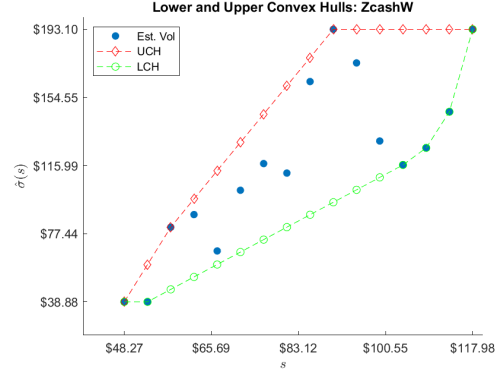


(b) Monero's Convex Hull Post-Filter

Figure 36: Zcash's Convex Hulls After Winsorizing Max & Min Points
(Date: 1/1/2019-7/17/2019)



(a) Zcash's Original Convex Hull

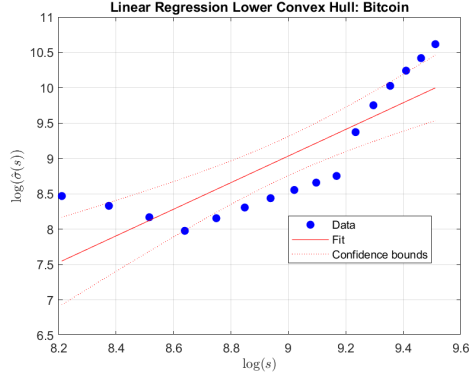


(b) Zcash's Convex Hull Post-Filter

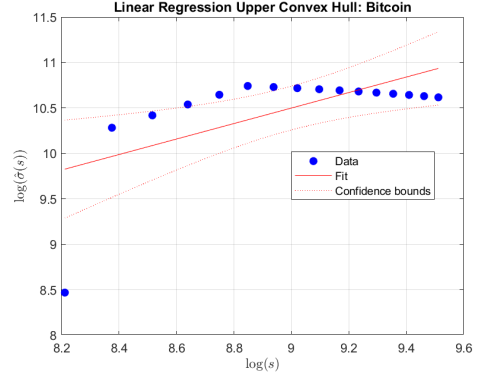
G Extrapolation (Cryptocurrency)

This section shows how power model is fit on each of the eight cryptocurrency's modified convex hulls. For demonstration, we provide both lower and upper convex hulls and their power fits. They are fit on the original estimated volatility and price pairs.

Figure 37: Estimation on Lower & Upper Convex Hulls: Bitcoin
(Date: 1/1/2019-7/17/2019)

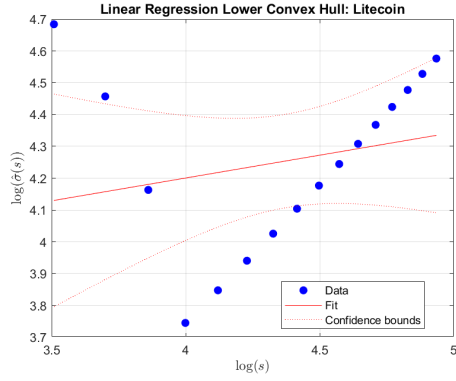


(a) Lower Convex Hull Estimation

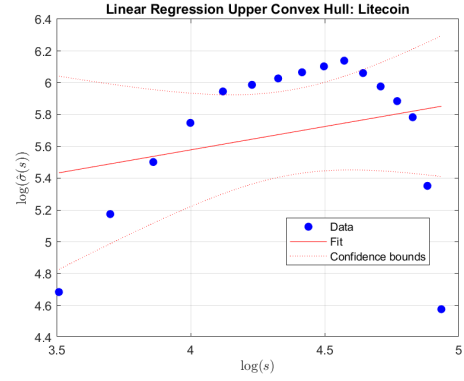


(b) Upper Convex Hull Estimation

Figure 38: Estimation on Lower & Upper Convex Hulls: Litecoin
(Date: 1/1/2019-7/17/2019)

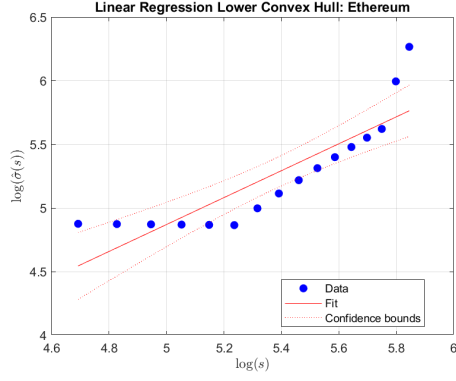


(a) Lower Convex Hull Estimation

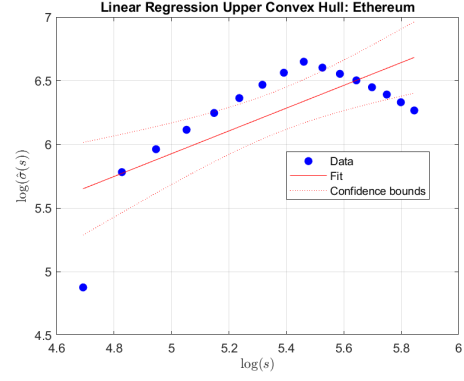


(b) Upper Convex Hull Estimation

Figure 39: Estimation on Lower & Upper Convex Hulls: Ethereum
(Date: 1/1/2019-7/17/2019)

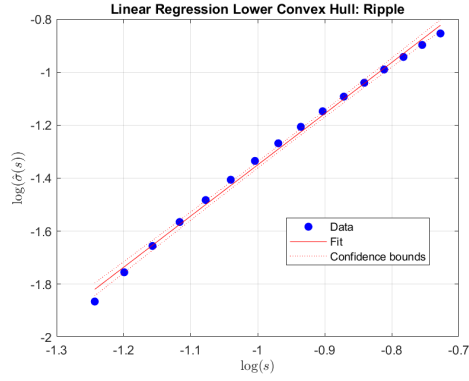


(a) Lower Convex Hull Estimation

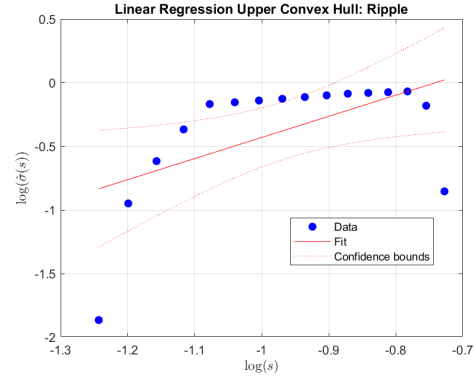


(b) Upper Convex Hull Estimation

Figure 40: Estimation on Lower & Upper Convex Hulls: Ripple
(Date: 1/1/2019-7/17/2019)

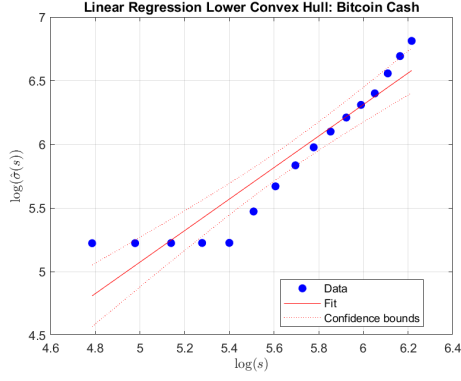


(a) Lower Convex Hull Estimation

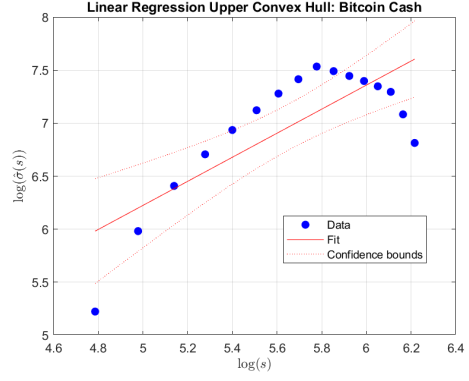


(b) Upper Convex Hull Estimation

Figure 41: Estimation on Lower & Upper Convex Hulls: Bitcoin Cash
(Date: 1/1/2019-7/17/2019)

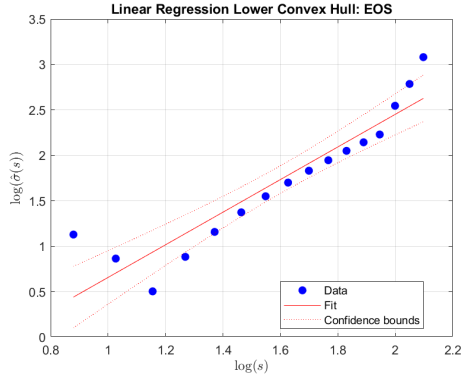


(a) Lower Convex Hull Estimation

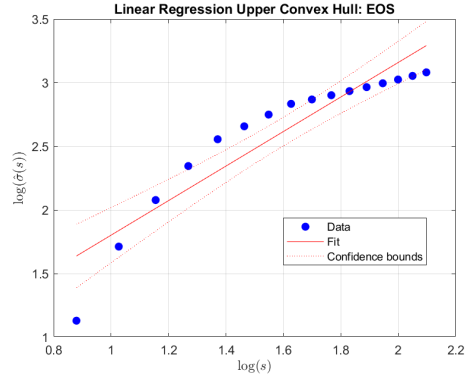


(b) Upper Convex Hull Estimation

Figure 42: Estimation on Lower & Upper Convex Hulls: EOS
(Date: 1/1/2019-7/17/2019)

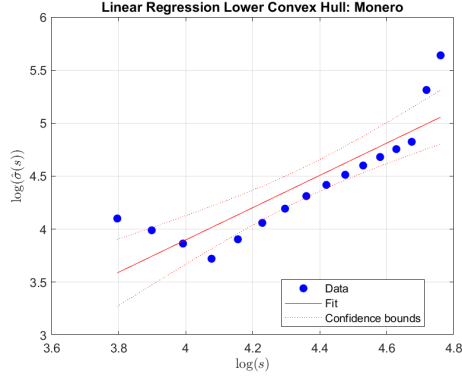


(a) Lower Convex Hull Estimation

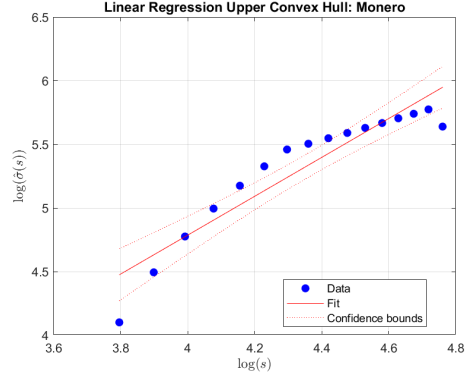


(b) Upper Convex Hull Estimation

Figure 43: Estimation on Lower & Upper Convex Hulls: Monero
(Date: 1/1/2019-7/17/2019)

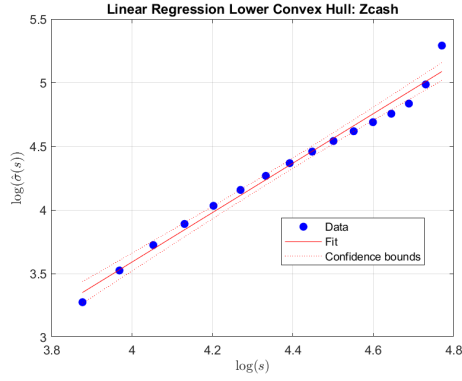


(a) Lower Convex Hull Estimation

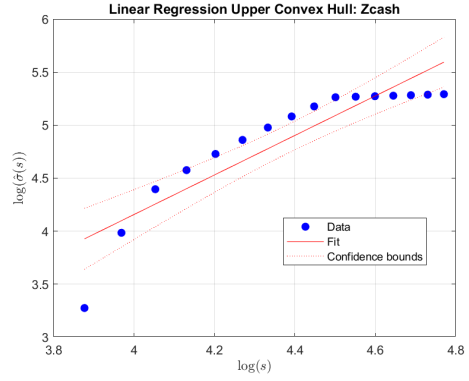


(b) Upper Convex Hull Estimation

Figure 44: Estimation on Lower & Upper Convex Hulls: Zcash
(Date: 1/1/2019-7/17/2019)



(a) Lower Convex Hull Estimation

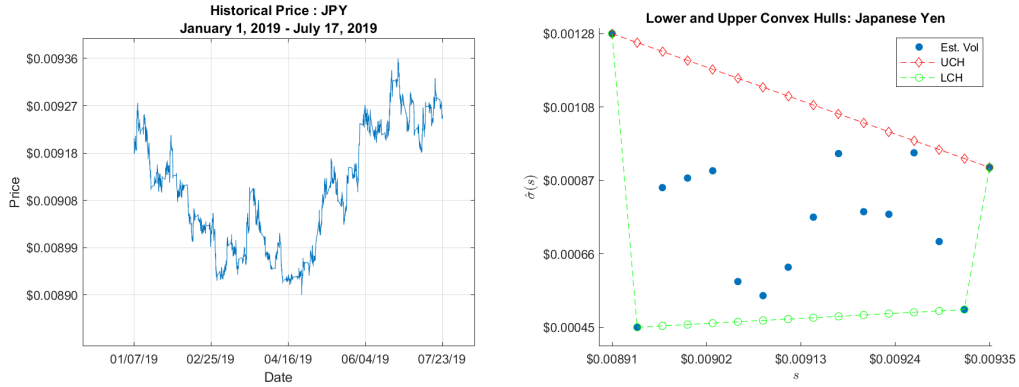


(b) Upper Convex Hull Estimation

H Interpolation (Foreign Currency)

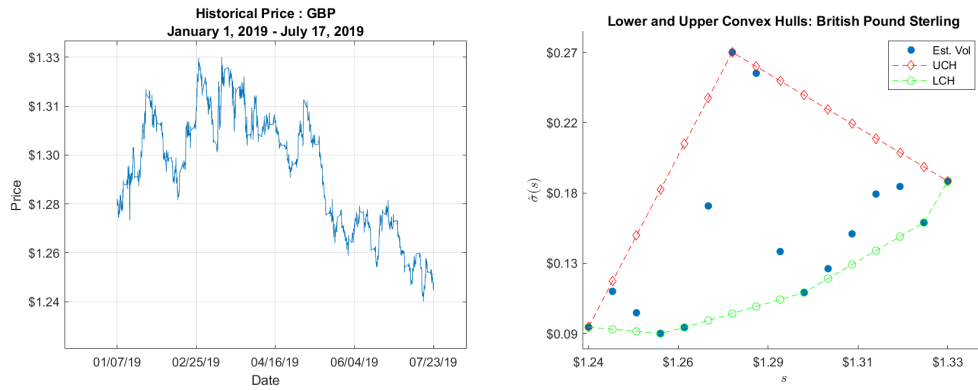
The figures in this section demonstrate how the modified upper and lower convex hulls are constructed for each foreign currency. They are constructed with the original points. There are total 3,457 observed hourly prices for each foreign exchange rate covering the dates from January 7, 2019 to July 23, 2019.

Figure 45: USD-JPY's Historical Exchange Rate & Estimated Volatility
(Date: 1/7/2019-7/23/2019)



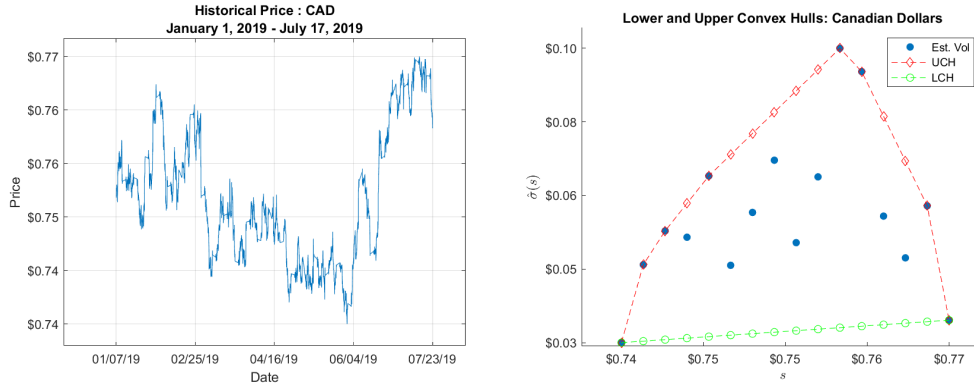
(a) USD-JPY **Hourly** Exchange Rates (b) Estimated Volatility for USD-JPY

Figure 46: USD-GBP's Historical Exchange Rate & Estimated Volatility
(Date: 1/7/2019-7/23/2019)



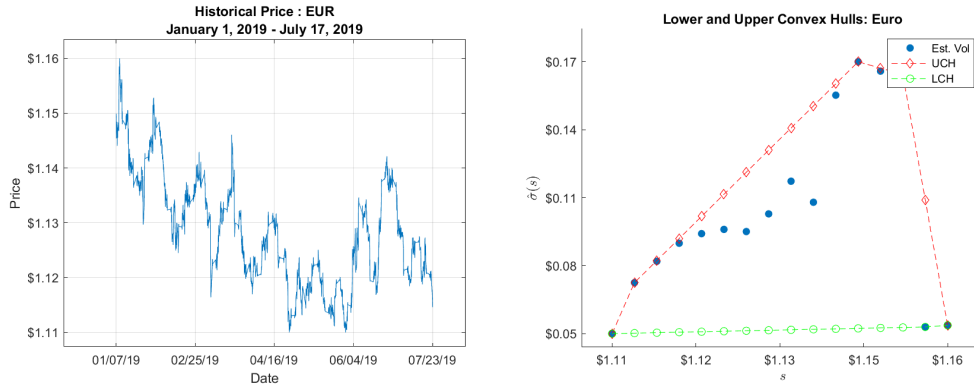
(a) USD-GBP **Hourly** Exchange Rates (b) Estimated Volatility for USD-GBP

Figure 47: USD-CAD's Historical Exchange Rate & Estimated Volatility
(Date: 1/7/2019-7/23/2019)



(a) USD-CAD **Hourly** Exchange Rates (b) Estimated Volatility for USD-CAD

Figure 48: USD-EUR's Historical Exchange Rate & Estimated Volatility
(Date: 1/7/2019-7/23/2019)

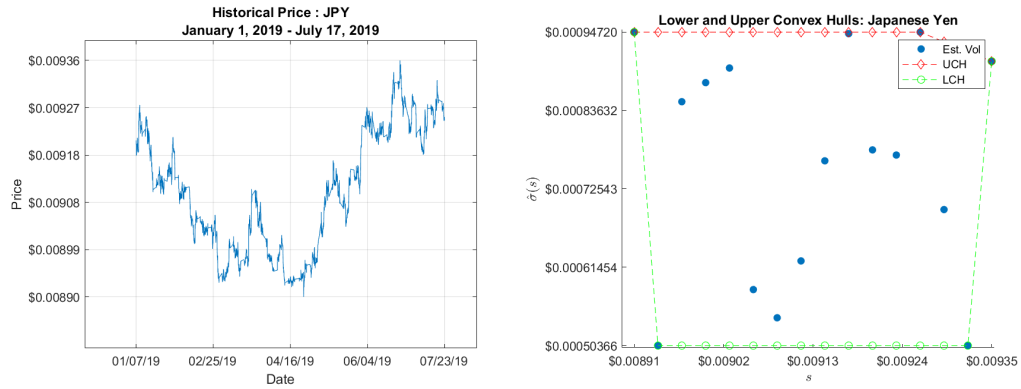


(a) USD-EUR **Hourly** Exchange Rates (b) Estimated Volatility for USD-EUR

I Interpolation (FOREX, Winsorized)

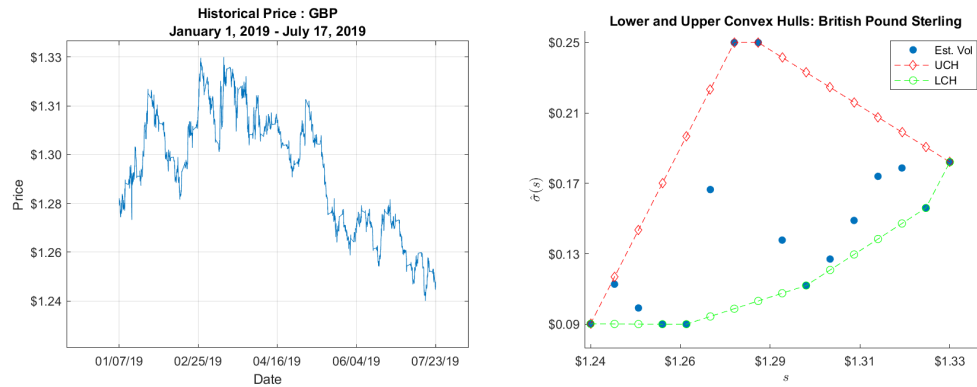
The figures in this section demonstrate how the modified upper and lower convex hulls are constructed for each foreign currency when the maximum and minimum volatility points are replaced with their second highest and lowest points. There are total 3,457 observed hourly prices for each foreign exchange rate covering the dates from January 7, 2019 to July 23, 2019.

Figure 49: USD-JPY's Historical Exchange Rate & Winsorized Convex Hull
(Date: 1/7/2019-7/23/2019)



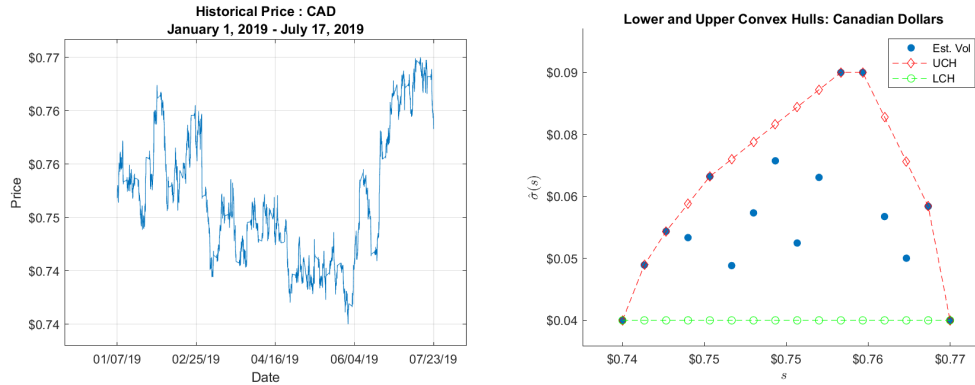
(a) USD-JPY **Hourly** Exchange Rates (b) Estimated Volatility for USD-JPY

Figure 50: USD-GBP's Historical Exchange Rate & Winsorized Convex Hull
(Date: 1/7/2019-7/23/2019)



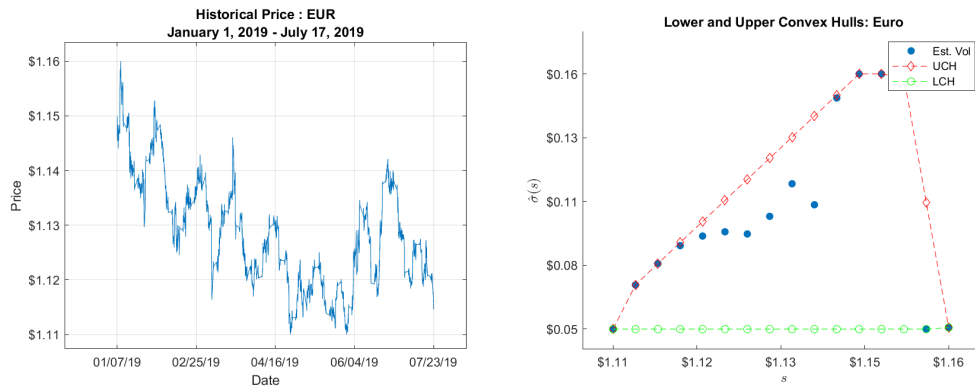
(a) USD-GBP **Hourly** Exchange Rates (b) Estimated Volatility for USD-GBP

Figure 51: USD-CAD's Historical Exchange Rate & Winsorized Convex Hull
(Date: 1/7/2019-7/23/2019)



(a) USD-CAD **Hourly** Exchange Rates (b) Estimated Volatility for USD-CAD

Figure 52: USD-EUR's Historical Exchange Rate & Winsorized Convex Hull
(Date: 1/7/2019-7/23/2019)

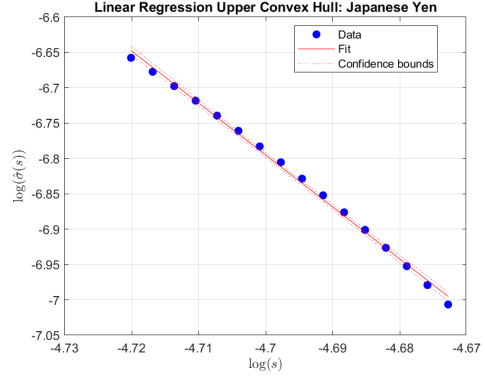
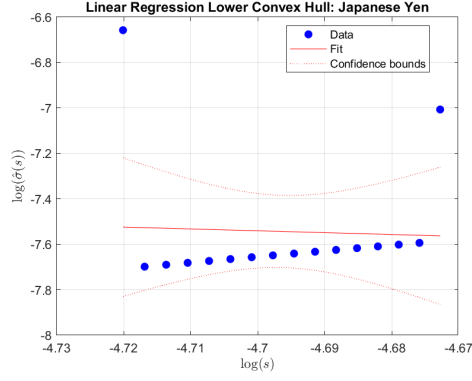


(a) USD-EUR **Hourly** Exchange Rates (b) Estimated Volatility for USD-EUR

J Extrapolation (Foreign Currency)

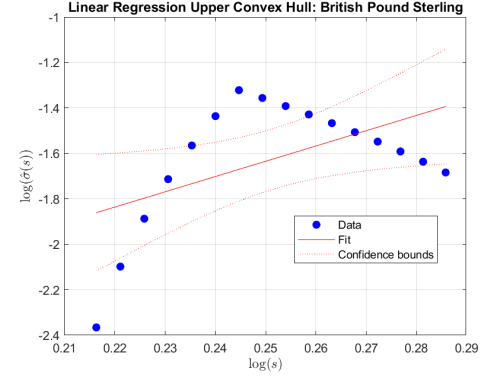
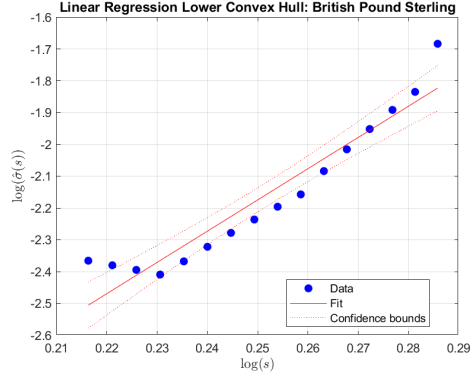
This section shows how power model is fit on each of the four foreign currencies' modified convex hulls. For demonstration, we provide both lower and upper convex hulls and their power fits. They are fit on the original estimated volatility and price pairs.

Figure 53: USD-JPY's Modified Convex Hull Regression
(Date: 1/7/2019-7/23/2019)



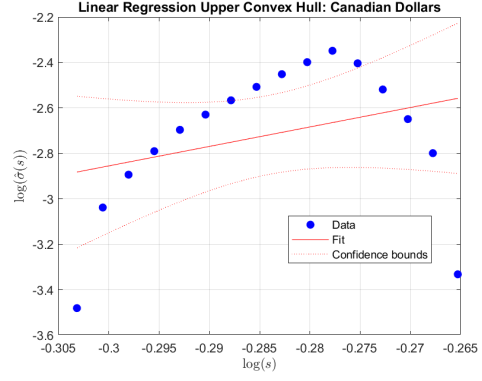
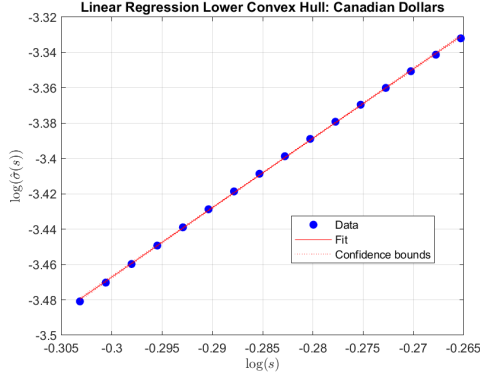
(a) USD-JPY: Lower Convex Hull Fit (b) USD-JPY: Upper Convex Hull Fit

Figure 54: USD-GBP's Modified Convex Hull Regression
(Date: 1/7/2019-7/23/2019)



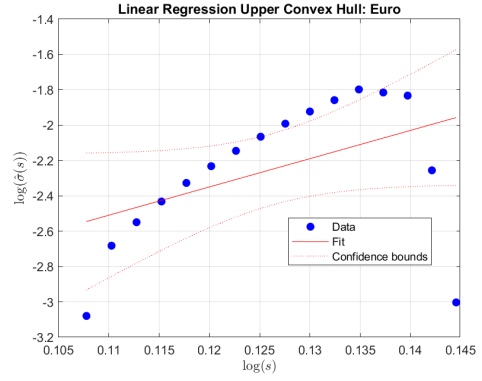
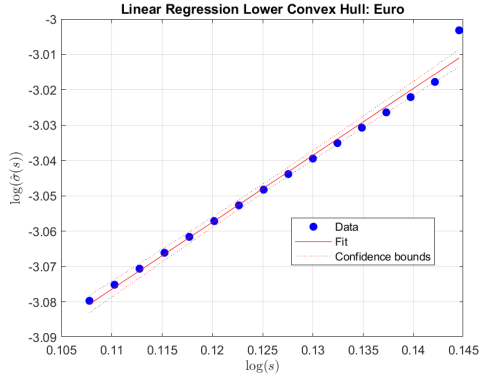
(a) USD-GBP: Lower Convex Hull Fit (b) USD-GBP: Upper Convex Hull Fit

Figure 55: USD-CAD's Modified Convex Hull Regression
(Date: 1/7/2019-7/23/2019)



(a) USD-CAD: Lower Convex Hull Fit (b) USD-CAD: Upper Convex Hull Fit

Figure 56: USD-EUR's Modified Convex Hull Regression
(Date: 1/7/2019-7/23/2019)



(a) USD-EUR: Lower Convex Hull Fit (b) USD-EUR: Upper Convex Hull Fit

K Extrapolation: Regression (Crypto, FOREX)

This section provides the full regression results for both cryptocurrencies and foreign exchange rates using MCHA and with the (unwinsorized) original estimated volatility and price points. It provides their estimates for the slope and constant of the power model and their associated t -statistic, p -value, standard errors, confidence intervals, and R^2 .

Regression (Power Model) Results: MCHA on Cryptocurrencies

Table 14: Lower Convex Hull using MCHA on Cryptocurrencies (Slope)

Currency	Slope	SE	t -stat	p -value	LowerCI	UpperCI	R^2
BTC	1.884	0.332	5.674	0.0001	1.172	2.596	69.69%
LTC	0.143	0.162	0.887	0.3900	-0.203	0.490	5.32%
ETH	1.058	0.161	6.581	0.0000	0.713	1.403	75.57%
XRP	1.932	0.035	55.728	0.0000	1.857	2.006	99.55%
BCH	1.238	0.117	10.617	0.0000	0.988	1.489	88.95%
EOS	1.795	0.195	9.213	0.0000	1.377	2.213	85.84%
XMR	1.523	0.235	6.483	0.0000	1.019	2.026	75.01%
ZEC	1.944	0.069	28.028	0.0000	1.795	2.092	98.25%

Table 15: Lower Convex Hull using MCHA on Cryptocurrencies (Intercept)

Currency	Intercept	SE	t -stat	p -value	LowerCI	UpperCI	R^2
BTC	-7.920	2.987	-2.651	0.0190	-14.327	-1.512	69.69%
LTC	3.627	0.711	5.102	0.0002	2.102	5.151	5.32%
ETH	-0.420	0.865	-0.485	0.6351	-2.275	1.436	75.57%
XRP	0.582	0.034	17.171	0.0000	0.509	0.654	99.55%
BCH	-1.117	0.661	-1.689	0.1133	-2.536	0.301	88.95%
EOS	-1.137	0.320	-3.555	0.0032	-1.824	-0.451	85.84%
XMR	-2.192	1.024	-2.141	0.0504	-4.388	0.004	75.01%
ZEC	-4.184	0.305	-13.733	0.0000	-4.837	-3.530	98.25%

Table 16: Upper Convex Hull using MCHA on Cryptocurrencies (Slope)

Currency	Slope	SE	<i>t</i> -stat	<i>p</i> -value	LowerCI	UpperCI	R^2
BTC	0.853	0.289	2.949	0.0106	0.233	1.473	38.32%
LTC	0.293	0.294	0.999	0.3348	-0.337	0.924	6.65%
ETH	0.895	0.223	4.016	0.0013	0.417	1.374	53.53%
XRP	1.660	0.668	2.486	0.0262	0.228	3.092	30.62%
BCH	1.135	0.238	4.759	0.0003	0.623	1.646	61.80%
EOS	1.358	0.144	9.439	0.0000	1.049	1.666	86.42%
XMR	1.528	0.152	10.064	0.0000	1.202	1.854	87.86%
ZEC	1.865	0.233	8.010	0.0000	1.365	2.364	82.09%

Table 17: Upper Convex Hull using MCHA on Cryptocurrencies (Intercept)

Currency	Intercept	SE	<i>t</i> -stat	<i>p</i> -value	LowerCI	UpperCI	R^2
BTC	2.826	2.601	1.086	0.2957	-2.753	8.405	38.32%
LTC	4.404	1.291	3.411	0.0042	1.635	7.174	6.65%
ETH	1.450	1.200	1.209	0.2468	-1.123	4.023	53.53%
XRP	1.230	0.653	1.884	0.0805	-0.170	2.630	30.62%
BCH	0.551	1.352	0.408	0.6895	-2.348	3.451	61.80%
EOS	0.444	0.236	1.880	0.0810	-0.062	0.951	86.42%
XMR	-1.326	0.662	-2.004	0.0649	-2.746	0.094	87.86%
ZEC	-3.302	1.023	-3.228	0.0061	-5.495	-1.108	82.09%

Regression (CEV Model) Results: Cryptocurrencies

Table 18: Convex Hull on Cryptocurrencies (Slope) using CEV

Currency	Slope	SE	t -stat	p -value	LowerCI	UpperCI	R^2
BTC	1.248	0.477	2.614	0.0204	0.224	2.271	32.80%
LTC	0.540	0.344	1.571	0.1386	-0.197	1.277	14.98%
ETH	1.030	0.309	3.329	0.0050	0.366	1.693	44.19%
XRP	1.849	0.589	3.141	0.0072	0.587	3.112	41.35%
BCH	1.146	0.291	3.938	0.0015	0.522	1.770	52.55%
EOS	1.435	0.297	4.837	0.0003	0.798	2.071	62.57%
XMR	1.771	0.292	6.073	0.0000	1.146	2.397	72.49%
ZEC	1.698	0.275	6.180	0.0000	1.109	2.287	73.18%

Table 19: Convex Hull on Cryptocurrencies (Intercept) using CEV

Currency	Intercept	SE	t -stat	p -value	LowerCI	UpperCI	R^2
BTC	-1.530	4.294	-0.356	0.7269	-10.740	7.680	32.80%
LTC	2.738	1.511	1.812	0.0915	-0.503	5.978	14.98%
ETH	0.336	1.664	0.202	0.8431	-3.234	3.905	44.19%
XRP	1.246	0.575	2.165	0.0482	0.012	2.479	41.35%
BCH	0.053	1.650	0.032	0.9749	-3.487	3.593	52.55%
EOS	-0.127	0.487	-0.261	0.7980	-1.172	0.917	62.57%
XMR	-2.882	1.272	-2.267	0.0398	-5.609	-0.155	72.49%
ZEC	-2.795	1.207	-2.316	0.0362	-5.383	-0.207	73.18%

Regression (Power Model) Results: MCHA on Foreign Currencies

Table 20: Lower Convex Hull on Foreign Currencies (Slope)

Currency	Slope	SE	<i>t</i> -stat	<i>p</i> -value	LowerCI	UpperCI	R^2
JPY	-0.817	5.097	-0.160	0.875	-11.749	10.116	0.18%
GBP	9.822	0.823	11.938	0.000	8.057	11.586	91.06%
CAD	3.928	0.016	246.754	0.000	3.894	3.962	99.98%
EUR	1.893	0.053	35.940	0.000	1.780	2.006	98.93%

Table 21: Lower Convex Hull on Foreign Currencies (Intercept)

Currency	Intercept	SE	<i>t</i> -stat	<i>p</i> -value	LowerCI	UpperCI	R^2
JPY	-11.378	23.938	-0.475	0.642	-62.721	39.964	0.18%
GBP	-4.630	0.208	-22.303	0.000	-5.075	-4.185	91.06%
CAD	-2.289	0.005	-505.570	0.000	-2.298	-2.279	99.98%
EUR	-3.285	0.007	-491.887	0.000	-3.299	-3.270	98.93%

Table 22: Upper Convex Hull on Foreign Currencies (Slope)

Currency	Slope	SE	<i>t</i> -stat	<i>p</i> -value	LowerCI	UpperCI	R^2
JPY	-7.352	0.106	-69.116	0.000	-7.580	-7.124	99.71%
GBP	6.725	2.912	2.310	0.037	0.481	12.970	27.60%
CAD	8.567	6.970	1.229	0.239	-6.382	23.515	9.74%
EUR	15.995	8.338	1.918	0.076	-1.888	33.878	20.82%

Table 23: Upper Convex Hull on Foreign Currencies (Intercept)

Currency	Intercept	SE	<i>t</i> -stat	<i>p</i> -value	LowerCI	UpperCI	R^2
JPY	-41.348	0.500	-82.774	0.000	-42.419	-40.277	99.71%
GBP	-3.316	0.735	-4.513	0.000	-4.891	-1.740	27.60%
CAD	-0.285	1.982	-0.144	0.888	-4.535	3.966	9.74%
EUR	-4.269	1.057	-4.039	0.001	-6.536	-2.002	20.82%

L Extrapolation: Regression (Crypto, Winsorized)

This section provides the full regression results for the winsorized set of estimated volatility and price pairs for cryptocurrencies. It provides their estimates for the slope and constant of the power model and their associated t -statistic, p -value, standard errors, confidence intervals, and R^2 .

Table 24: Winsorized Lower Convex Hull
MCHA on Cryptocurrencies (Slope)

Currency	Slope	SE	95 CR	R^2	t -stat	p -value	LowerCI	UpperCI
BTC	1.785	0.306	1.503	70.89%	5.839	0.0000	1.008	2.422
LTC	0.034	0.057	1.093	2.49%	0.598	0.5596	-0.105	0.142
ETH	1.055	0.159	1.261	75.87%	6.635	0.0000	0.682	1.193
XRP	0.193	0.005	1.008	99.09%	39.058	0.0000	0.194	0.207
BCH	1.237	0.117	1.192	88.88%	10.577	0.0000	0.791	1.527
EOS	1.395	0.097	1.159	93.68%	14.400	0.0000	1.010	1.416
XMR	1.368	0.188	1.310	79.02%	7.262	0.0000	0.815	1.631
ZEC	1.661	0.071	1.116	97.54%	23.554	0.0000	1.557	1.690

Table 25: Winsorized Lower Convex Hull
MCHA on Cryptocurrencies (Intercept)

Currency	Intercept	SE	t -stat	p -value	LowerCI	UpperCI	R^2
BTC	-6.97329	2.751182	-2.146	0.0530	-12.674	0.096	69.69%
LTC	4.325832	0.2497	17.645	0.0000	3.867	4.956	5.32%
ETH	-0.39786	0.855217	0.586	0.5687	-1.007	1.748	75.57%
XRP	-0.71757	0.004826	-235.991	0.0000	-0.717	-0.704	99.55%
BCH	-1.10759	0.663038	-0.649	0.5284	-2.733	1.478	88.95%
EOS	-0.37761	0.159098	-0.090	0.9297	-0.346	0.318	85.84%
XMR	-1.42662	0.820986	-0.952	0.3601	-2.550	1.000	75.01%
ZEC	-2.89044	0.309892	-20.343	0.0000	-3.042	-2.454	98.25%

Table 26: Winsorized Upper Convex Hull
MCHA on Cryptocurrencies (Slope)

Currency	Slope	SE	95 CR	R^2	t -stat	p -value	LowerCI	UpperCI
BTC	0.854	0.273	0.552	41.24%	3.135	0.0073	0.343	1.509
LTC	0.240	0.271	0.555	5.32%	0.887	0.3900	-0.390	0.860
ETH	0.859	0.181	0.703	61.70%	4.749	0.0003	0.483	1.266
XRP	0.767	0.433	0.288	18.35%	1.774	0.0979	-0.597	1.781
BCH	1.196	0.187	0.692	74.51%	6.398	0.0000	0.632	1.418
EOS	1.157	0.174	0.713	75.85%	6.631	0.0000	0.765	1.666
XMR	1.407	0.159	0.738	84.76%	8.825	0.0000	1.075	1.861
ZEC	1.632	0.172	0.716	86.48%	9.464	0.0000	0.779	2.088

Table 27: Winsorized Upper Convex Hull
MCHA on Cryptocurrencies (Intercept)

Currency	Intercept	SE	t -stat	p -value	LowerCI	UpperCI	R^2
BTC	2.753	2.452	0.817	0.4301	-3.293	7.240	38.32%
LTC	4.580	1.190	3.597	0.0037	1.793	7.301	6.65%
ETH	1.542	0.973	1.466	0.1683	-0.690	3.528	53.53%
XRP	0.452	0.423	0.520	0.6128	-0.877	1.426	30.62%
BCH	0.068	1.060	0.977	0.3477	-1.240	3.257	61.80%
EOS	0.694	0.286	1.786	0.0994	-0.133	1.339	86.42%
XMR	-0.841	0.695	-1.410	0.1839	-2.816	0.603	87.86%
ZEC	-2.256	0.757	-1.078	0.3021	-4.304	1.454	82.09%

M Extrapolation: Regression (FOREX, Winsorized)

This section provides the regression results for the winsorized set of estimated volatility and price pairs for foreign exchange rates. It provides their estimates for the slope and constant of the power model and their associated t -statistic, p -value, standard errors, confidence intervals, and R^2 .⁸

⁸Note the Canadian Dollar rates produce a zero slope with its winsorized lower convex hull which is a horizontal line. The divergent t -stats for the Canadian Dollar in Table 28 and 29 reflect this.

Table 28: Winsorized Lower Convex Hull
MCHA on Foreign Currencies (Slope)

Currency	Slope	SE	t -stat	p -value	LowerCI	UpperCI	R^2
JPY	-0.375	3.706	-0.101	0.921	-8.322	7.573	0.07%
GBP	9.549	0.829	11.515	0.000	7.771	11.328	90.45%
CAD	0.000	0.000	∞	0.000	0.000	0.000	100.00%
EUR	0.131	0.076	1.720	0.107	-0.032	0.293	17.45%

Table 29: Winsorized Lower Convex Hull
MCHA on Foreign Currencies (Intercept)

Currency	Intercept	SE	t -stat	p -value	LowerCI	UpperCI	R^2
JPY	-9.276	17.403	-0.533	0.602	-46.601	28.049	0.07%
GBP	-4.556	0.209	-21.774	0.000	-5.005	-4.108	90.45%
CAD	-3.332	0.000	$-\infty$	0.000	-3.332	-3.332	100.00%
EUR	-3.033	0.010	-315.156	0.000	-3.054	-3.013	17.45%

Table 30: Winsorized Upper Convex Hull
MCHA on Foreign Currencies (Slope)

Currency	Slope	SE	t -stat	p -value	LowerCI	UpperCI	R^2
JPY	-0.562	0.179	-3.148	0.007	-0.945	-0.179	41.45%
GBP	7.123	2.776	2.566	0.022	1.169	13.077	31.99%
CAD	7.077	6.321	1.120	0.282	-6.480	20.634	8.22%
EUR	15.367	8.051	1.909	0.077	-1.900	32.634	20.65%

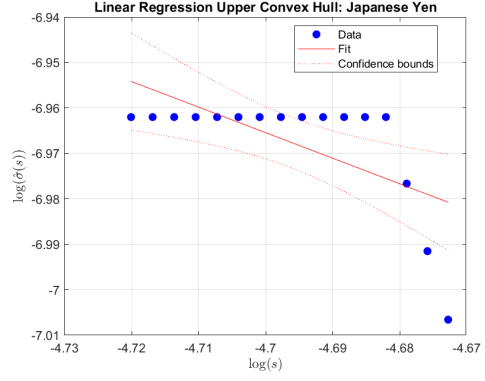
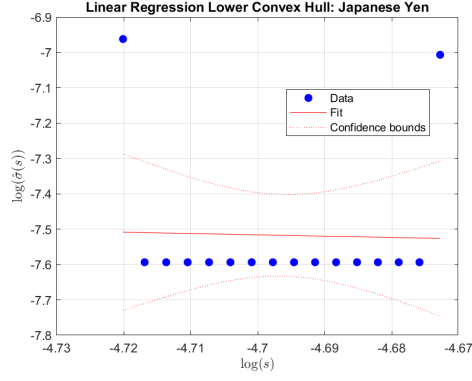
Table 31: Winsorized Upper Convex Hull
MCHA on Foreign Currencies (Intercept)

Currency	Intercept	SE	t -stat	p -value	LowerCI	UpperCI	R^2
JPY	-9.608	0.839	-11.454	0.000	-11.408	-7.809	41.45%
GBP	-3.435	0.701	-4.903	0.000	-4.937	-1.932	31.99%
CAD	-0.712	1.797	-0.396	0.698	-4.567	3.143	8.22%
EUR	-4.197	1.021	-4.112	0.001	-6.386	-2.008	20.65%

N Extrapolation (FOREX, Winsorized)

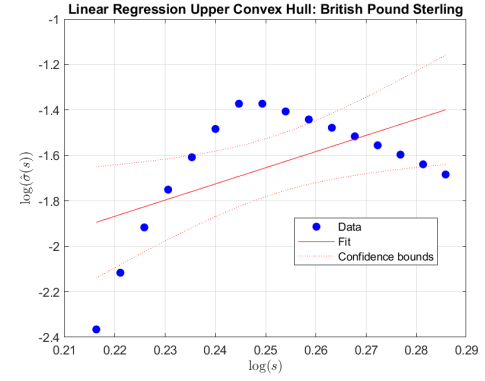
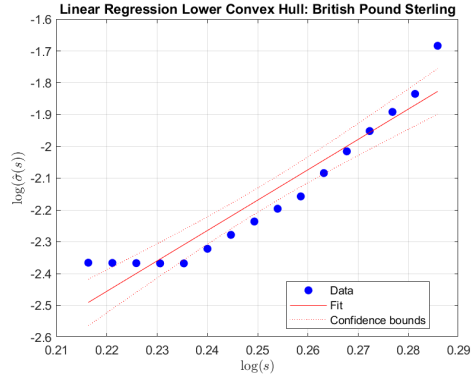
This section shows how power model is fit on each of the four foreign currencies' modified convex hulls. For demonstration, we provide both lower and upper convex hulls and their power fits. They are fit on the winsorized estimated volatility and price pairs.

Figure 57: USD-JPY's Winsorized Convex Hull Regression
(Date: 1/7/2019-7/23/2019)



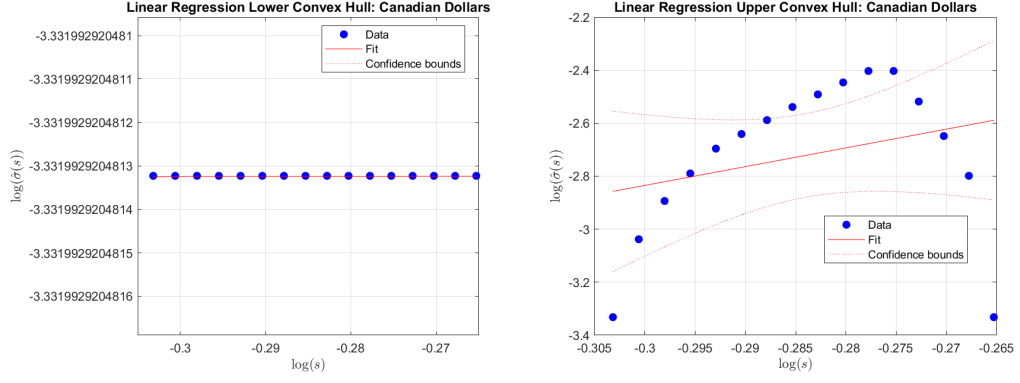
(a) USD-JPY: Lower Convex Hull Fit (b) USD-JPY: Upper Convex Hull Fit

Figure 58: USD-GBP's Winsorized Convex Hull Regression
(Date: 1/7/2019-7/23/2019)



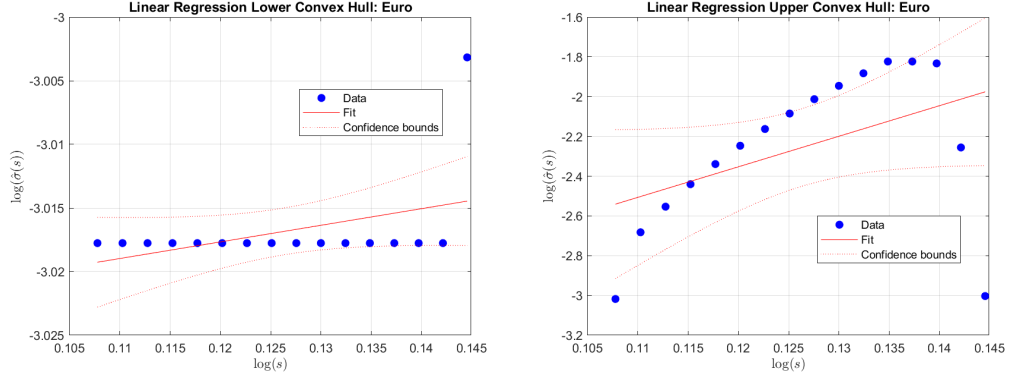
(a) USD-GBP: Lower Convex Hull Fit (b) USD-GBP: Upper Convex Hull Fit

Figure 59: USD-CAD's Winsorized Convex Hull Regression
(Date: 1/7/2019-7/23/2019)



(a) USD-CAD: Lower Convex Hull Fit (b) USD-CAD: Upper Convex Hull Fit

Figure 60: USD-EUR's Winsorized Convex Hull Regression
(Date: 1/7/2019-7/23/2019)

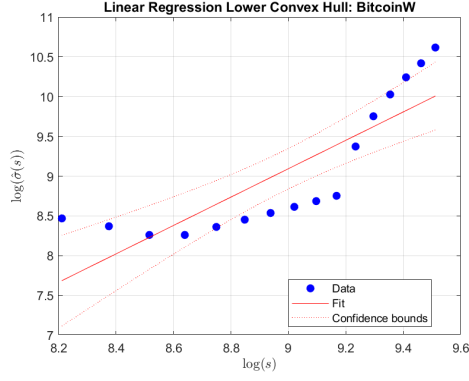


(a) USD-EUR: Lower Convex Hull Fit (b) USD-EUR: Upper Convex Hull Fit

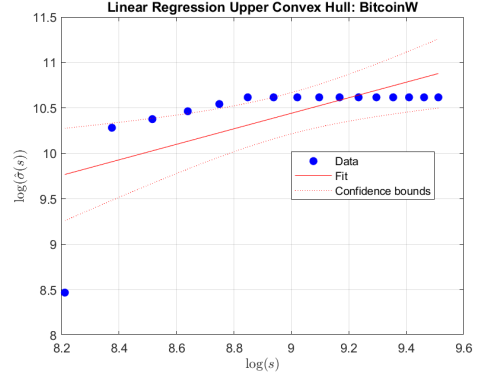
O Extrapolation (Crypto, Winsorized)

This section shows how power model is fit on each of the eight cryptocurrencies' modified convex hulls. For demonstration, we provide both lower and upper convex hulls and their power fits. They are fit on the winsorized estimated volatility and price pairs.

Figure 61: Estimation on Winsorized Convex Hulls: Bitcoin
(Date: 1/1/2019-7/17/2019)

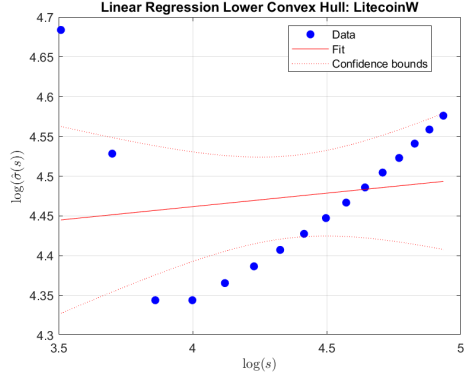


(a) Lower Convex Hull Estimation

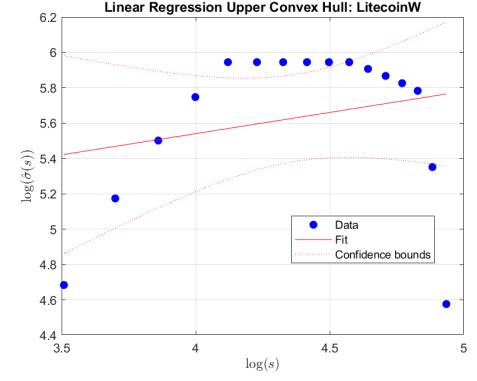


(b) Upper Convex Hull Estimation

Figure 62: Estimation on Winsorized Convex Hulls: Litecoin
(Date: 1/1/2019-7/17/2019)

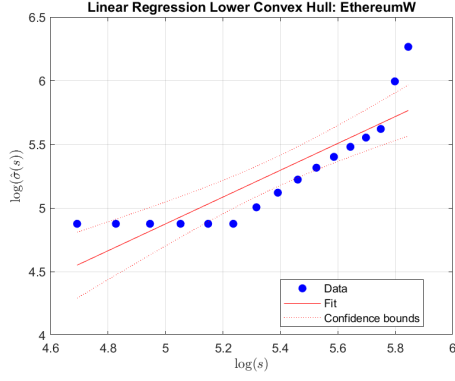


(a) Lower Convex Hull Estimation

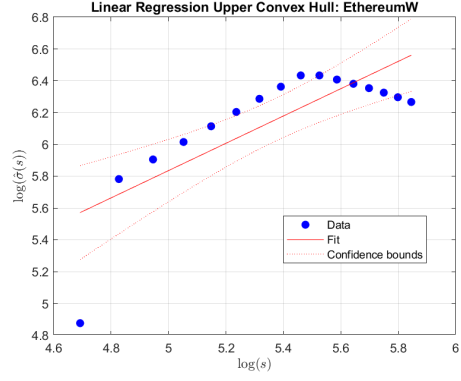


(b) Upper Convex Hull Estimation

Figure 63: Estimation on Winsorized Convex Hulls: Ethereum
(Date: 1/1/2019-7/17/2019)

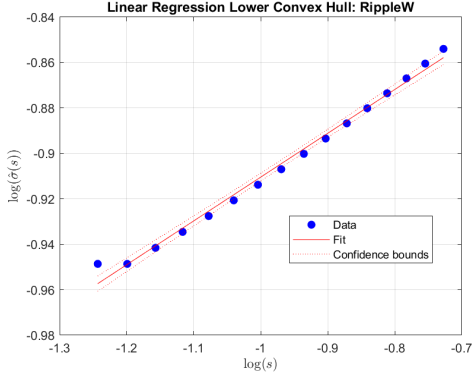


(a) Lower Convex Hull Estimation

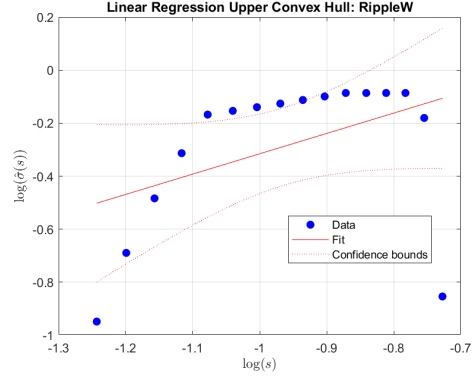


(b) Upper Convex Hull Estimation

Figure 64: Estimation on Winsorized Convex Hulls: Ripple
(Date: 1/1/2019-7/17/2019)

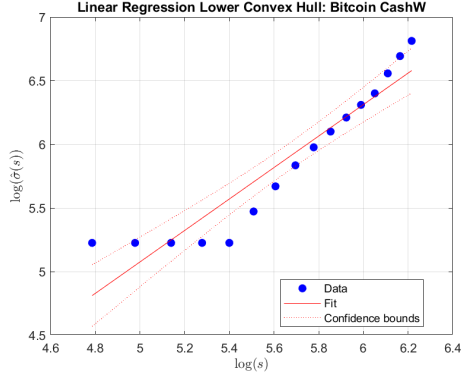


(a) Lower Convex Hull Estimation

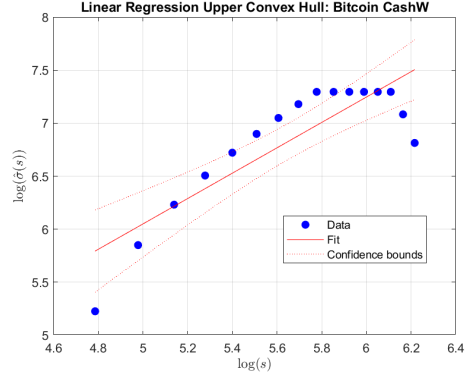


(b) Upper Convex Hull Estimation

Figure 65: Estimation on Winsorized Convex Hulls: Bitcoin Cash
(Date: 1/1/2019-7/17/2019)

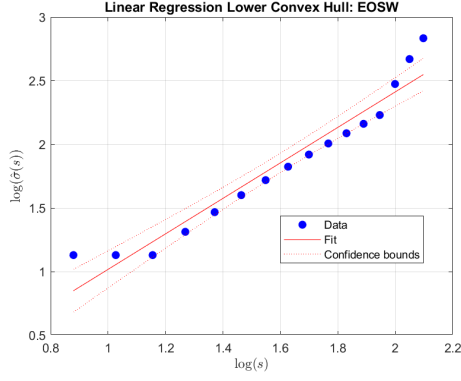


(a) Lower Convex Hull Estimation

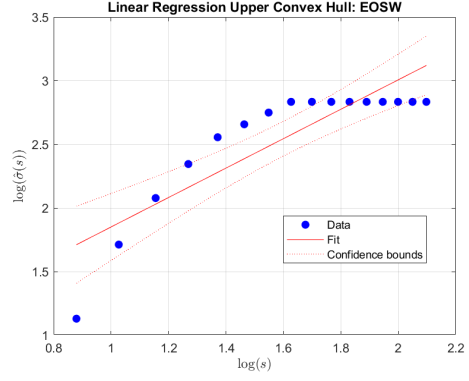


(b) Upper Convex Hull Estimation

Figure 66: Estimation on Winsorized Convex Hulls: EOS
(Date: 1/1/2019-7/17/2019)

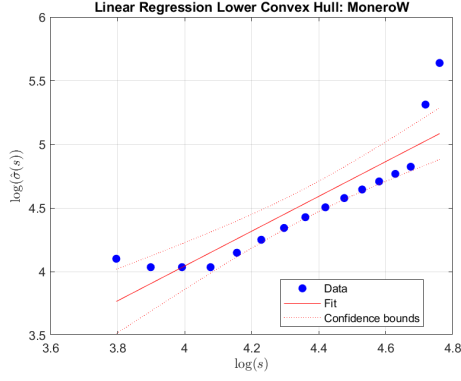


(a) Lower Convex Hull Estimation

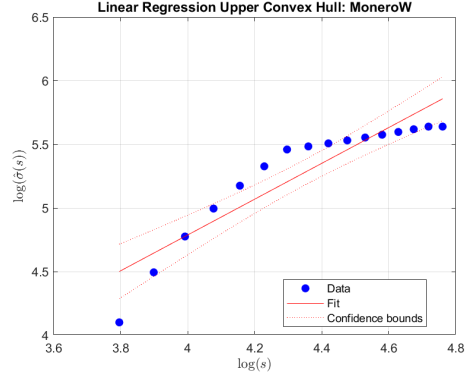


(b) Upper Convex Hull Estimation

Figure 67: Estimation on Winsorized Convex Hulls: Monero
(Date: 1/1/2019-7/17/2019)

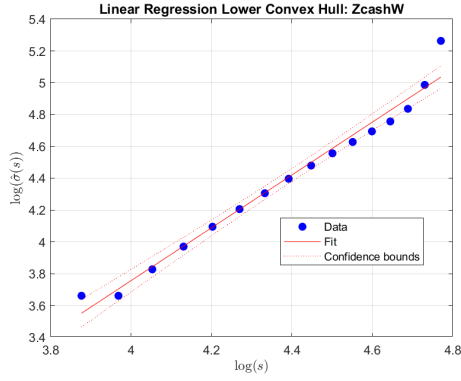


(a) Lower Convex Hull Estimation

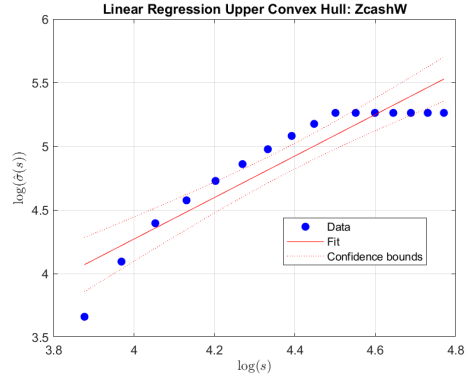


(b) Upper Convex Hull Estimation

Figure 68: Estimation on Winsorized Convex Hulls: Zcash
(Date: 1/1/2019-7/17/2019)



(a) Lower Convex Hull Estimation



(b) Upper Convex Hull Estimation